



**HAL**  
open science

## River signature over coastal area (Eastern Mediterranean): Grain size and geochemical analyses of sediments

Myriam Ghsoub, Milad Fakhri, Thierry Courp, Gaby Khalaf, Roselyne Buscail, Wolfgang Ludwig

### ► To cite this version:

Myriam Ghsoub, Milad Fakhri, Thierry Courp, Gaby Khalaf, Roselyne Buscail, et al.. River signature over coastal area (Eastern Mediterranean): Grain size and geochemical analyses of sediments. *Regional Studies in Marine Science*, 2020, 35, pp.101169 -. 10.1016/j.rsma.2020.101169 . hal-03490089

**HAL Id: hal-03490089**

**<https://hal.science/hal-03490089>**

Submitted on 22 Aug 2022

**HAL** is a multi-disciplinary open access archive for the deposit and dissemination of scientific research documents, whether they are published or not. The documents may come from teaching and research institutions in France or abroad, or from public or private research centers.

L'archive ouverte pluridisciplinaire **HAL**, est destinée au dépôt et à la diffusion de documents scientifiques de niveau recherche, publiés ou non, émanant des établissements d'enseignement et de recherche français ou étrangers, des laboratoires publics ou privés.



Distributed under a Creative Commons Attribution - NonCommercial 4.0 International License

# 1 River signature over coastal area (Eastern Mediterranean):

## 2 Grain size and geochemical analyses of sediments

3 Myriam Ghsoub (a, b), Milad Fakhri (a), Thierry Courp (b), Gaby Khalaf (a), Roselyne Buscail (b), and Wolfgang  
4 Ludwig (b)

5 (a) Lebanese National Council for Scientific Research – National Centre for Marine Sciences (CNRS-L/CNSM) Lebanon (bihar@cnrs.edu.lb),  
6 (b) Université de Perpignan Via Domitia, Centre de Formation et de Recherche sur les Environnements Méditerranéens, UMR 5110, 52 Avenue Paul Alduy, 66860, Perpignan,  
7 France (cefrem@univ-perp.fr)

### 8 9 10 Abstract

11 Rivers and coastal areas are two ecosystems in permanent interaction. Thus, to understand the  
12 process occurring at the land-sea continuum, the determination of the origin and fate of sediment  
13 and its associated organic matter is critical. Moreover, tracing the source of particulate matter  
14 from terrestrial origin has not been adequately carried out in the eastern Mediterranean basin,  
15 especially in Lebanon. In order to differentiate between the terrestrial and marine sources of  
16 particulate matter and characterize the depositional environments, grain size composition,  
17 organic carbon (OC), total nitrogen (TN), Isotopic Ratio ( $\delta^{13}\text{C}$ ), the terrestrial and labile fractions  
18 of organic matter, as well as, photosynthetic pigments were analyzed for surface sediment  
19 samples collected from the coastal marine area facing the mouth of Ibrahim river and from the  
20 river watershed.

21 This study shows that the combined use of the grain size composition of sediments and carbon  
22 isotopic signatures ( $\delta^{13}\text{C}$ ) of its associated organic matter is an efficient tool to track the source  
23 and fate of organic matter in highly dynamic estuarine and coastal ecosystems.

24 The obtained results illustrate the occurrence of two grain size compositional types associated  
25 with two different depositional environments. Shallow stations ( $\leq 30$  m) are characterized by a  
26 hydrological sorting and strong hydrodynamic conditions leading to the winnowing of the finer  
27 fraction to deep stations ( $\geq 60$  m) found to be impacted by river inputs.

28 Organic carbon and total nitrogen values are strongly correlated with the mud fraction  
29 controlling their distribution, and therefore leading to their accumulation in the sediment of deep  
30 stations ( $\geq 60$  m). On the other hand,  $\delta^{13}\text{C}$  values and terrestrial fraction percentage suggest the

1 occurrence of riverine materials at the stations ( $\geq 60$  m), while at the shallow stations, addition of  
2 local autochthonous production materials occurs associated with high values of chlorophyll and  
3 labile organic matter fraction.

4 **Keywords:** Eastern Mediterranean, Estuary, Sediments, Grain size,  $\delta^{13}\text{C}$  isotopic ratio, Organic  
5 carbon.

## 6 **1. Introduction**

7 Coastal areas are dynamic zones where interaction occurs between land, air and water. Due to  
8 the instability at these transitional areas, sediment characteristics are significantly varying from  
9 those occurring offshore. In fact, this instability in the environmental conditions that is controlled  
10 by waves and currents affects the composition of sediments and its associated parameters, as  
11 well as, their distribution and dispersal (Kulkarni et al., 2015).

12 Coastal sediments generally consist of organic and inorganic particles that reach the coastal zone  
13 by different pathways. Particle size analysis is widely applied in environmental studies and used  
14 to reveal the origin of sediments, as well as, their deposition and transport mechanisms. In fact,  
15 the particle size composition of sediments is closely related to the energetic and hydrodynamic  
16 conditions governing the depositional environments (Zhong et al., 2017), since each environment  
17 is described by its own particle size characteristics (Baiyegunhi et al., 2017). Particle size  
18 distribution is also influenced by several factors such as particle origin, climatic conditions and  
19 topography (Abuodha, 2003).

20 Furthermore, organic matter in all its aspects plays a central role in marine ecosystems as a  
21 potential food resource (Fabiano and Danovaro, 1994). Its concentration in surface sediments  
22 reflects the amount of food available to the benthic communities. It is affected by sediment  
23 characteristics, especially grain size, and it is divided into two fractions: a refractory fraction and  
24 a labile fraction. Therefore, in order to estimate the amount of available organic matter for benthic

1 consumers, biochemical classes (lipids, proteins and carbohydrates) must be analyzed since the  
2 quantity of organic matter evaluated by the amount of total organic carbon is considered as an  
3 overestimation of food availability. During the transport of organic matter from shallower to deeper  
4 waters, its labile fraction decreases due to mineralization while the refractory part remains  
5 present. Thus, at deeper marine areas acting as depositional environments, organic matter is  
6 mainly composed of a refractory fraction (Incera et al., 2003; Winogradow and Pempkowiak,  
7 2018).

8 Those organic compounds may derive from marine and freshwater plankton and benthos, as well  
9 as, terrestrial matter transported by rivers. Therefore, in order to reveal the origin of organic  
10 matter, the  $\delta^{13}\text{C}$  isotopic ratio may be analyzed and the contribution of each source may be  
11 estimated (Li et al., 2016). In addition, terrestrial organic matter is characterized by more depleted  
12  $\delta^{13}\text{C}$  (with a typical range of : -25 to -33‰) than marine organic matter (with a typical range of : -  
13 18 to -22‰) (Ranjan et al., 2011; Li et al., 2016; Winogradow and Pempkowiak, 2018). In order  
14 to assess the proportions of terrestrial organic carbon in surface marine sediments, a  $\delta^{13}\text{C}$  two  
15 end-member model may be applied based on the assumption of  $\delta^{13}\text{C}$  values for terrestrial and  
16 marine end-member carbon (Liu et al., 2015; Li et al., 2016).

17 At marine areas, organic matter is well preserved in the low energy environments associated to  
18 finer grain size fractions while primary production occurs at shallow areas near the shoreline  
19 characterized by higher nutrient inputs and strong hydrodynamic conditions. Hence, as an  
20 important indicator of primary production, chlorophyll-a concentrations may be analyzed  
21 (Winogradow and Pempkowiak, 2018; Zhang and Blomquist, 2018). In fact, the analysis of  
22 photosynthetic pigments is used to study microphytobenthos communities, particularly in surface  
23 layers where photosynthesis occurs and therefore, where marine productivity can be estimated  
24 (Magni et al., 2000).

1 Several studies are carried out worldwide at the land-sea continuum focusing on grain size and  
2 geochemical analysis (Mohan, 2000 ; Rajganapathi et al., 2013; Kulkarni et al., 2015; Ramesh et  
3 al., 2015 ; Abballe and Chivas, 2017 ; Padhi et al., 2017; Zhong et al., 2017; Wang et al., 2018 ;  
4 Winogradow and Pempkowiak, 2018) and in the western Mediterranean, specifically at the Gulf  
5 of Lion (Higuera, 2014 ; Pruski et al., 2019). Fewer studies are conducted in the eastern  
6 Mediterranean namely at the Greek (Karageorgis et al., 2000) and Lebanese coasts (Fakhri et  
7 al., 2008 ; 2018). Indeed, the majority of the studies focused on the watersheds of the Lebanese  
8 coastal rivers: El Kabir River by Thomas et al., (2005), El Bared River by Khalaf et al., (2009), al  
9 Jaouz River by Nakhlé, (2003) and Khalaf et al., (2007), Antelias River by Saad et al., (2004a)  
10 and among the southern coastal rivers: Damour and Awali Rivers by Saad et al., (2004b),  
11 Hasbani-Wazzani River by Tarabay, (2011) and the longest Lebanese river, Litani River by  
12 Nehme et al., (2014) and Mcheik et al., (2015). Furthermore, several studies were executed on  
13 the Ibrahim River watershed by Khalaf, (1984); Korfali and Davies, (2003); Nakhlé, (2003);  
14 Assaker, (2016) and El Najjar et al., (2019).

15 Being one of the largest Lebanese coastal rivers, characterized by the highest flow among the  
16 Lebanese rivers (408 million m<sup>3</sup>/ year) (Fitzpatrick et al., 2001 ; Assaker, 2016), it will be relevant  
17 and interesting to choose the Ibrahim River as a case study in order to estimate the sediment  
18 inputs and river contribution in the marine environment.

19 Thus, this study aims to investigate the sediment characteristics and dispersal, as well as, the  
20 associated organic matter distribution and sources at the coastal zone facing Ibrahim River Mouth  
21 (North of Beirut, Lebanon). It acts as a case study of the eastern Mediterranean basin where  
22 studies using a combination of grain size composition of sediments and bulk properties of organic  
23 matter including the carbon isotopic ratio ( $\delta^{13}\text{C}$ ) are limited. However, due to the complexity of the  
24 coastal environment characteristics, such multiple approaches combining granulometric and  
25 geochemical analyses are important.

## 1 **2. Material and Methods**

### 2 **2.1. Area of study**

3 Located in the eastern Mediterranean basin, at the base of Mount Lebanon chain, the Lebanese  
4 coastline (220 km) is characterized by a narrow continental shelf with an average width of 3-5 Km  
5 and an average depth of 20-40 m (Emery et al., 1966; Goedicke, 1973). Being parallel to Mount  
6 Lebanon, the continental shelf is oriented from the southwest to northeast and its western limit is  
7 defined by a strong slope at 100-200 m. As part of the warmest basin of the Mediterranean, the  
8 Lebanese coast is governed by a Mediterranean climate marked by two distinct seasons: a  
9 smooth winter and a hot and long dry summer promoting the precipitation of carbonates  
10 (Sanlaville, 1977).

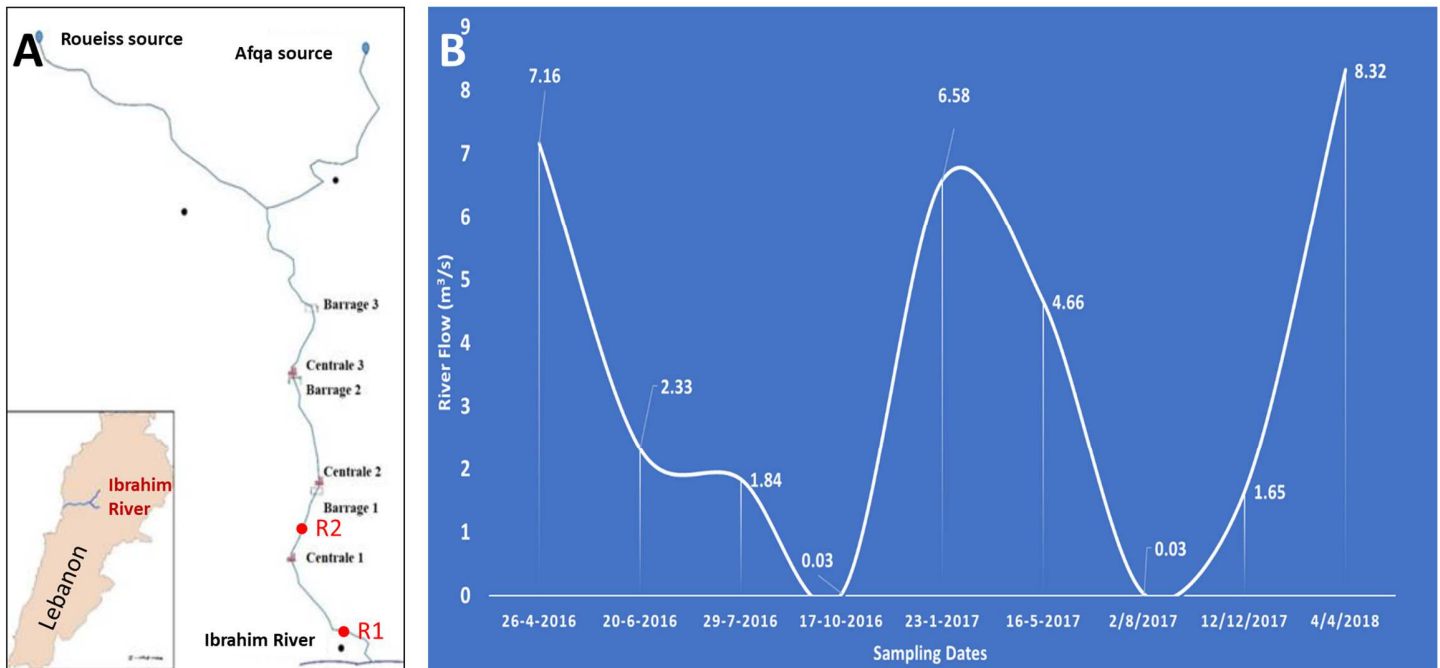
11 Over coastal areas, wind and currents are two main factors affecting the dispersion of suspended  
12 particles and bed sediments. Along the Lebanese coast, the prevailing winds are those of the  
13 western sector (southwest or northwest) (Abboud-Abi Saab, 1985). Open and unsheltered, the  
14 Lebanese coast is subjected to the prevailing winds and swell. Even in calm weather, a regular  
15 swell characterizes Lebanese surface waters especially observed in summer, and during winter  
16 the brutal and violent wave action activates the mechanical erosions of the coast (Nakhlé, 2003).  
17 The general circulation of surface waters along the Lebanese coast is South-North and the local  
18 coastal currents would be considered as simple ramifications of the general offshore currents,  
19 running perpendicularly to the coastline, toward the east in an anticyclonic circulation, and being  
20 affected by the topography of the continental shelf (Goedicke, 1973).

21 Small perennial coastal rivers discharge into the sea all along the coast with varying amplitudes  
22 affected by seasons and the geomorphology of the coastal zone (Abboud-Abi Saab et al., 2012).  
23 Furthermore, several submarine canyons are identified as extensions of valleys and continental  
24 rivers between Beirut and Batroun, such as, at the studied coastal area in front of the Ibrahim

1 River (Figure 2). These canyons are usually nearshore in the narrow continental shelf, thus,  
2 considered as traps for terrestrial particles, being directly transported to 1500 m (Elias, 2006).

3 Nowadays, the Lebanese coastal zone is subject to overexploitation and several sources of  
4 pollution, such as, industrial, agricultural and residential effluents, or other anthropogenic  
5 activities. In fact, 4 commercial ports, 15 fishing harbors, dozens of sea pipelines and various  
6 industries are located along the Lebanese shoreline. Moreover, about 53 wastewater outfalls are  
7 identified along the Lebanese coast which extend only a couple of meters or terminate at the  
8 water surface. The Lebanese shoreline is also affected by dumpsites and landfills near big cities  
9 such as Dora and Borj Hammoud, Tripoli, Sidon, and Tyre. These dumpsites destroy the coastal  
10 ecosystems by spreading solid wastes over the surface water and sea bottom  
11 (MOE/UNDP/ECODIT, 2011).

12 Ibrahim River, also known as the Adonis River, is a Lebanese coastal river with two main sources:  
13 El Roueiss at 1300 m altitude and Afqa at 1200 m altitude. This river (27 km long) flows into the  
14 sea 25 km north of Beirut draining a watershed with accentuated relief. It is characterized by a  
15 torrential regime, higher flow occurring between January and June (rainy period), and can be  
16 divided into three parts with different slope values: 14% at the upper part, 3% at the intermediate  
17 one and 2.5% at the lower part. Ibrahim River is interrupted by three dams that feed three  
18 hydroelectric power stations along its watercourse. Water is channeled from one dam to another  
19 affecting river flow (Figure 1 A). The catchment area is 326 Km<sup>2</sup>. It includes agricultural lands and  
20 is dominated by permeable limestone (Khalaf, 1984). The mean annual flow of Ibrahim River from  
21 September 1991 to August 2012 was 10,88 m<sup>3</sup>/s (Assaker, 2016). It decreased to 5.396 m<sup>3</sup> /s  
22 from September 2015 to August 2016 then increased to 8.758 m<sup>3</sup> /s from September 2016 to  
23 August 2017. The river flow during each sampling date is summarized in Figure 1 B.



2 **Figure 1:** Ibrahim River watershed and Dams

4 Ibrahim River flow during sampling dates (**B**)

3 location (Khalaf, 1984) (**A**)

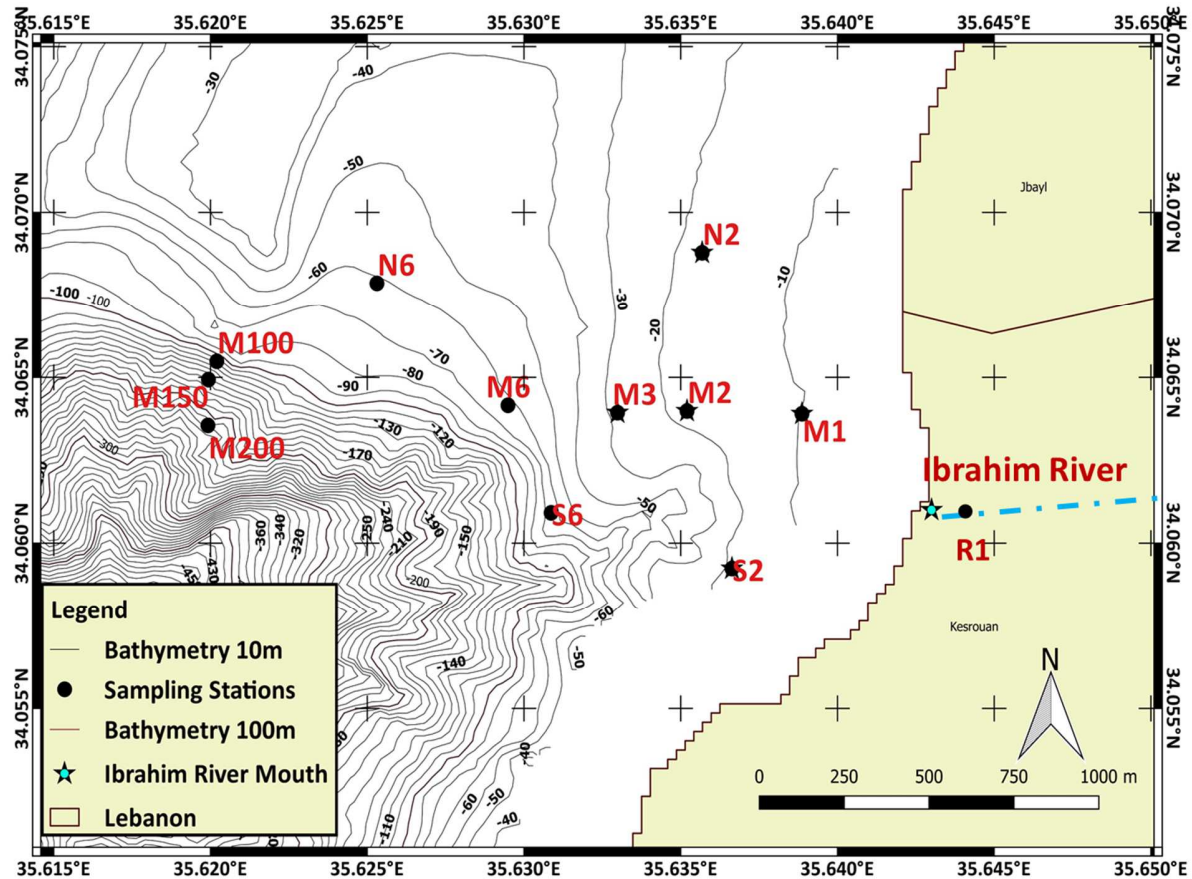
## 5 **2.2. Sampling**

6 Nine sampling campaigns were conducted at the coastal marine area facing Ibrahim River mouth  
 7 using the platform of the Lebanese scientific vessel “CANA-CNRS”. Sediment samples were  
 8 collected for two years from April 2016 to April 2018 (Figure 2) following three sampling transects  
 9 (Table 1 and Figure 2) (a southern transect: S; a middle transect: M; and a northern transect: N),  
 10 at seven different depths (10, 20, 30, 60, 100, 150, and 200 m), in total 11 stations, using a Van-  
 11 Veen grab and PVC corers. The upper 1 cm sediment layer was preserved and transferred into  
 12 pre-cleaned glass containers for organic analysis and plastic ones for chemical analysis.  
 13 Sediment samples were also collected from the river mouth (R1) and from the packed sediment  
 14 at the first dam (R2) (Figure 1 A).

1 **Table 1:** Description of the sampling stations (Depth and geographic location).

| Description                     | Stations | Depth | Transect | Coordinates                  |
|---------------------------------|----------|-------|----------|------------------------------|
| Marine surface sediment samples | M1       | 10 m  | Middle   | 34.06390 ° N<br>35.63887 ° E |
|                                 | M2       | 20 m  | Middle   | 34.06398 ° N<br>35.63520 ° E |
|                                 | M3       | 30 m  | Middle   | 34.06393 ° N<br>35.63298 ° E |
|                                 | M6       | 60 m  | Middle   | 34.06416 ° N<br>35.62949 ° E |
|                                 | M100     | 100 m | Middle   | 34.06548 ° N<br>35.62020 ° E |
|                                 | M150     | 150 m | Middle   | 34.06493 ° N<br>35.61993 ° E |
|                                 | M200     | 200 m | Middle   | 34.06355 ° N<br>35.61992 ° E |
|                                 | N2       | 20 m  | Northern | 34.06878 ° N<br>35.63568 ° E |
|                                 | N6       | 60 m  | Northern | 34.06786 ° N<br>35.62531 ° E |
|                                 | S2       | 20 m  | Southern | 34.05923 ° N<br>35.63663 ° E |
|                                 | S6       | 60 m  | Southern | 34.06091 ° N<br>35.63086 ° E |
| River surface sediment samples  | R1       |       |          | 34.06443 ° N<br>35.64465 ° E |
|                                 | R2       |       |          | 34.08283 ° N<br>35.68321 ° E |

2



1

2 **Figure 2:** Sampling stations distribution at Ibrahim River coastal marine area.

3 **2.3. Methods of analysis**

4 2.3.1. Grain size analysis:

5 Particle grain size analysis for sediments less than 2 mm was done using a Laser Scattering  
 6 Particle Size Distribution Analyzer (Partica LA-950V2) and followed by ultrasonic disaggregation.  
 7 This machine allows to accomplish the fastest analysis of grain size distribution based on laser  
 8 diffraction. The range detected by this machine is between 10 nm and 3000 µm allowing precise  
 9 measurements.

10

11 The results of the grain size composition were processed using the “Gradistat V8.0” Software to  
 12 calculate statistical parameters (Blott and Pye, 2001). “Triplot” software was used to generate the

1 trivariate plot. Passega diagram (Passega, 1964) or C-M plot were also used to reveal the  
2 hydrodynamic forces governing sediment transport and deposition in the studied area. It consists  
3 of plotting “C” ( $\mu\text{m}$ ): D99 coarser one percentile value and “M” ( $\mu\text{m}$ ): D50: the median value on a  
4 logarithmic scale.

5 The linear discriminant function (LDF) (Table 2) is a quantitative method usually used to  
6 differentiate among different environments and mediums of deposition. This method is based on  
7 the fact that each environment of deposition is characterized by its particular energy conditions  
8 reflected by the grain size distribution of sediments (Sahu, 1964).

9 Formulas for mean size (M), variance ( $r^2$ ), skewness (SK), and kurtosis (KG) deducted from Folk  
10 and Ward, (1957) are the most suitable (mutually independent, do not require normal  
11 distributions) to be used for this analysis (Sahu, 1964). The average grain size (mean size) of the  
12 sediments ( $\Phi = -\log_2 d$ ,  $d$ : size (mm)) was calculated and indicated the prevailing energy  
13 conditions (Manivel et al., 2016). The standard deviation of the mean (sorting) is a measure of  
14 uniformity in the particle size distribution reflecting the fluctuations of the energetic and  
15 hydrodynamic conditions governing the deposition medium (Grenier, 2014; Baiyegunhi et al.,  
16 2017; Padhi et al., 2017).

17 Skewness was used to differentiate between symmetrical distribution, the presence of a coarser  
18 tail (negative) or finer tail (positive) as an indicator of sub-population mixing (Ramesh et al., 2015;  
19 Manivel et al., 2016). Kurtosis was used to evaluate the sorting of the tail in comparison with the  
20 center of the curve. The distribution is Leptokurtic when the tail is better sorted in opposition to  
21 the Platykurtic distribution. The distribution is Mesokurtic when uniform sorting occurs between  
22 the tail and central part.

1 In order to study the total indications of the combined grain size parameters and, thus, reveal the  
 2 environment of deposition, a multivariate analysis of sediments granulometry was used based on  
 3 the following formulae (Table 2),(Kulkarni et al., 2015; Padhi et al., 2017).

4 **Table 2:** Linear discriminant functions to differentiate among environment of depositions

| <b>Environments and processes discrimination</b>                        | <b>Equation</b>  | <b>Indication</b>  |
|---|--|--|
| <b>Between “Aeolian process” and “Littoral environment”:</b>            | $Y_1 = -3.5688M + 3.7016r^2 - 2.0766SK + 3.1135KG$ (Eq.1)    | $Y_1 > -2.7411$ would indicate littoral environment while $Y_1 < -2.7411$ would refer to an aeolian process.           |
| <b>Between “Littoral environment” and “Shallow marine environment”:</b> | $Y_2 = 15.6534M + 65.7091r^2 + 18.1071SK + 18.5043KG$ (Eq.2) | $Y_2 > 63.3650$ would refer to a shallow marine environment while $Y_2 < 63.3650$ would indicate littoral environment. |
| <b>Between “Shallow marine environment” and “Fluvial process”:</b>      | $Y_3 = 0.2852M - 8.7604r^2 - 4.8932SK + 0.0428KG$ (Eq.3)     | $Y_3 > -7.4190$ : would refer to a shallow marine environment while $Y_3 < -7.4190$ would indicate a fluvial process.  |
| <b>Between “Fluvial process” and “Turbidity current process”</b>        | $Y_4 = 0.7215M - 0.4030r^2 + 6.7322SK + 5.2927KG$ (Eq.4)     | $Y_4 < 9.8433$ would indicate turbidity current process and $Y_4 > 9.8433$ would refer to a fluvial process.           |

5

6 -To differentiate between “aeolian process” and “littoral environment”, Eq.1 is applied:

7  $Y_1 = -3.5688M + 3.7016r^2 - 2.0766SK + 3.1135KG$  (Eq.1)

8  $Y_1 < -2.7411$  reports an “aeolian process” and  $Y_1 > -2.7411$  refers to a “littoral environment”

9 -Eq.2 is applied to distinguish between “Littoral” and “Shallow marine” environments:

10  $Y_2 = 15.6534M + 65.7091r^2 + 18.1071SK + 18.5043KG$  (Eq.2)

11 When  $Y_2$  is  $< -63.3650$ , the environment is “Littoral” and when  $Y_2$  is  $> -63.3650$ , the environment

12 is “shallow marine”.

13 -To discriminate between the “fluvial process” and the “shallow marine environment”, Eq.3 is

14 applied:

15  $Y_3 = 0.2852M - 8.7604r^2 - 4.8932SK + 0.0428KG$  (Eq.3)

16  $Y_3 > -7.4190$  indicates a “shallow marine” environment while  $Y_3 < -7.4190$  refers to a “fluvial

17 process”.

1 -Eq.4 is applied to differentiate between “fluvial” and “turbidity current” deposits:

$$2 \quad Y_4 = 0.7215M - 0.4030r^2 + 6.7322Sk + 5.2927KG \quad (\text{Eq.4})$$

3  $Y_4 < 9.8433$  refers to “turbidity current” deposits while  $Y_4 > 9.8433$  refers to “fluvial” deposits.

4 Using the discriminant functions, it is then possible to discriminate among processes (aeolian,  
5 marine, fluvial, and turbidity current) and environments of deposition (littoral and shallow agitated  
6 marine).

7 Moreover, once those discriminant functions are applied to a sample or population, the  
8 environment or process of deposition may be deduced depending on whether the value  
9 approaches towards the first side (the first environment) or towards the second side (the second  
10 environment) (Sahu, 1964 in Kulkarni et al., 2015 ; Baiyegunhi et al., 2017 ; Padhi et al., 2017).

11 Prior to the following analysis, sediment samples were crushed using a Planetary Ball Mill PM  
12 200 RETSCH at CEFREM Laboratories.

### 13 2.3.2. $\delta^{13}\text{C}$ Isotopic Ratio

14 Samples are decarbonated by repeated additions of HCl (2N), rinsed with cold deionized water  
15 before freeze-drying (Schubert and Nielsen, 2000). An elemental analyzer “Eurovector 3000”  
16 coupled to a mass spectrometer “Isoprime” (EA-IRMS) was used and the isotopic results are given  
17 by the following equation:

18  $\delta^{13}\text{C} = [(R_{\text{sample}}/R_{\text{standard}}) - 1] * 1000$ , with R:  $^{13}\text{C}/^{12}\text{C}$  and the standard is the international Vienna  
19 Pee Dee Belemnite (PDB).  $\delta^{13}\text{C}$  values are reported as per thousand (‰). All samples were  
20 analyzed twice and the analytical precision was better than 0.2‰.

21 A two end-members model of organic matter  $\delta^{13}\text{C}$  signatures was used to estimate the OC  
22 terrestrial fraction (Ft) following this equation (Li et al., 2016):

$$23 \quad Ft = [(\delta^{13}\text{C}_{\text{marine}} - \delta^{13}\text{C}_{\text{sample}}) / (\delta^{13}\text{C}_{\text{marine}} - \delta^{13}\text{C}_{\text{terrestrial}})] * 100 \quad (\text{Eq.5})$$

1 The terrestrial  $\delta^{13}\text{C}$  end-member ( $\delta^{13}\text{C}_{\text{terrestrial}}$ ) was chosen based on R1 and R2 values (river  
2 stations) -27‰ while the chosen marine end member ( $\delta^{13}\text{C}_{\text{marine}}$ ) -21‰ (ranging from -21.6 to -  
3 20.3‰) based on the values taken from marine organism (plankton and benthos) (Li et al., 2016;  
4 Wang et al., 2018).

### 5 2.3.3. Total Nitrogen (TN)

6 TN was measured by combustion in an automatic elemental analyzer (Elementar Vario MAX CN).

7 The calibrations were made with a Soil certified standard. TN was expressed in % of the sample  
8 dry weight with a precision of 5 to 10% depending on the concentration.

### 9 2.3.4. Organic Carbon (OC)

10 Total organic carbon was analyzed by adopting the simple titration method approved by the  
11 Expertise Centre in Environmental Analysis of Québec (M.A., 2010). OC was expressed in % of  
12 the sample dry weight with a precision of 20% and a quantification limit of 0.1%.

### 13 2.3.5. Labile Organic matter fraction (LOM)

14 Carbohydrates (CHO) were measured according to Brink et al. (1960) method at 625 nm  
15 (maximum absorbance), and compared to a glucose standard curve. The method of Barnes and  
16 Blackstock (1973) was used for the determination of lipids (LPD) at a wavelength of 520 nm, and  
17 the concentrations were calculated in comparison to cholesterol standards. Protein (PRT)  
18 estimation was accomplished by applying the method of Stevenson and Cheng (1970). The  
19 absorbance was read at  $\lambda$ : 570 nm, compared with a L-alanine standard curve.

20 The labile fraction of organic matter is the sum of CHO, LPD, and PRT. Its proportion was  
21 expressed as a percentage of TOC (CLOM/TOC%) after the conversion of CHO, PRT and LPD  
22 into carbon equivalents using the conversion factors 0.40, 0.49, and 0.75, respectively (Fabiano  
23 and Danovaro, 1994 in Tselepides et al., 2000).

### 1 2.3.6. Photosynthetic Pigments

2 Chlorophyll-*a* and phaeopigments were extracted according to the method described by  
3 Lorenzen, (1967) and modified by Magni et al., (2000). The extraction of the photosynthetic  
4 pigments was executed by adding 90% acetone to the sample. Spectrophotometric analysis was  
5 executed after 24 hours (in dark), before acidification for chlorophyll-*a* and after acidification for  
6 phaeopigments.

### 8 2.3.7. Statistical Analyses

9 Statistical analysis was performed using R software. A Schapiro-Wilk test was used to test the  
10 normality of the measured variables. A Kruskal Wallis followed by a Dunn-test test were employed  
11 to reveal differences between sampling sites and sampling seasons. Moreover, in order to  
12 elucidate the relations between the parameters and regroup the sampling stations that share the  
13 same characteristics at the studied zone, a principal component analysis was applied.

14 Principal Component Analysis (PCA) is a multivariate descriptive analysis used to reduce the size  
15 of the initial data matrix with a minimum deformation of the reality, in other words, obtain the most  
16 relevant summary of the data. Using a correlation matrix, the dispersion of data was analyzed by  
17 extracting a reduced number of factors which replaced the initial variables and were used to plot  
18 the required distribution graphs to easily understand the data distribution (individuals or stations  
19 and variables or studied parameters) (Besse, 1992).

## 20 **3. Results**

### 21 **3.1. Grain size analysis over Ibrahim River coastal area:**

22 3.1.1. Mean size: An increase of the mean grain size ( $\Phi$ ) was noticed seawards, sandy  
23 sediments shifting to silty sediments at deep stations (Figure 3 A). The shallow near shore stations  
24 (M1, M2, M3, N2, S2) occurring between 10 and 30 m depth were mainly composed of fine sand

1 (2-3 phi) as shown by the ternary diagram (Figure 4 A), ranging from 60 to 90%, in opposition to  
2 the stations occurring between 60 and 200 m depth mainly constituted of fine fraction (Mud: >4  
3 phi) from 70 to 90% (Stations: M6, N6, S6, M100, M150, M200).

4 3.1.2. Standard deviation (Sorting): Shallow stations ( $\leq 30$  m) were moderately well to moderately  
5 sorted while the deep stations ( $\geq 60$  m) were poorly to very poorly sorted (Figure 3 B).

6 3.1.3. Skewness: The sediment samples of the studied area followed a symmetrical to very fine  
7 skewed distribution (Figure 3 C). At the near shore shallow stations ( $\leq 30$  m), distribution was  
8 symmetrical, while at the deep stations ( $\geq 60$  m), distribution was fine to very finely skewed.

9 3.1.4. Kurtosis: The sediment samples of the studied area were characterized by Mesokurtic to  
10 very Leptokurtic distribution indicating the occurrence of one dominant population and another  
11 subordinate in the studied region (Ramesh et al., 2015; Manivel et al., 2016).

12 3.1.5. CM Diagram (Passega Diagram):

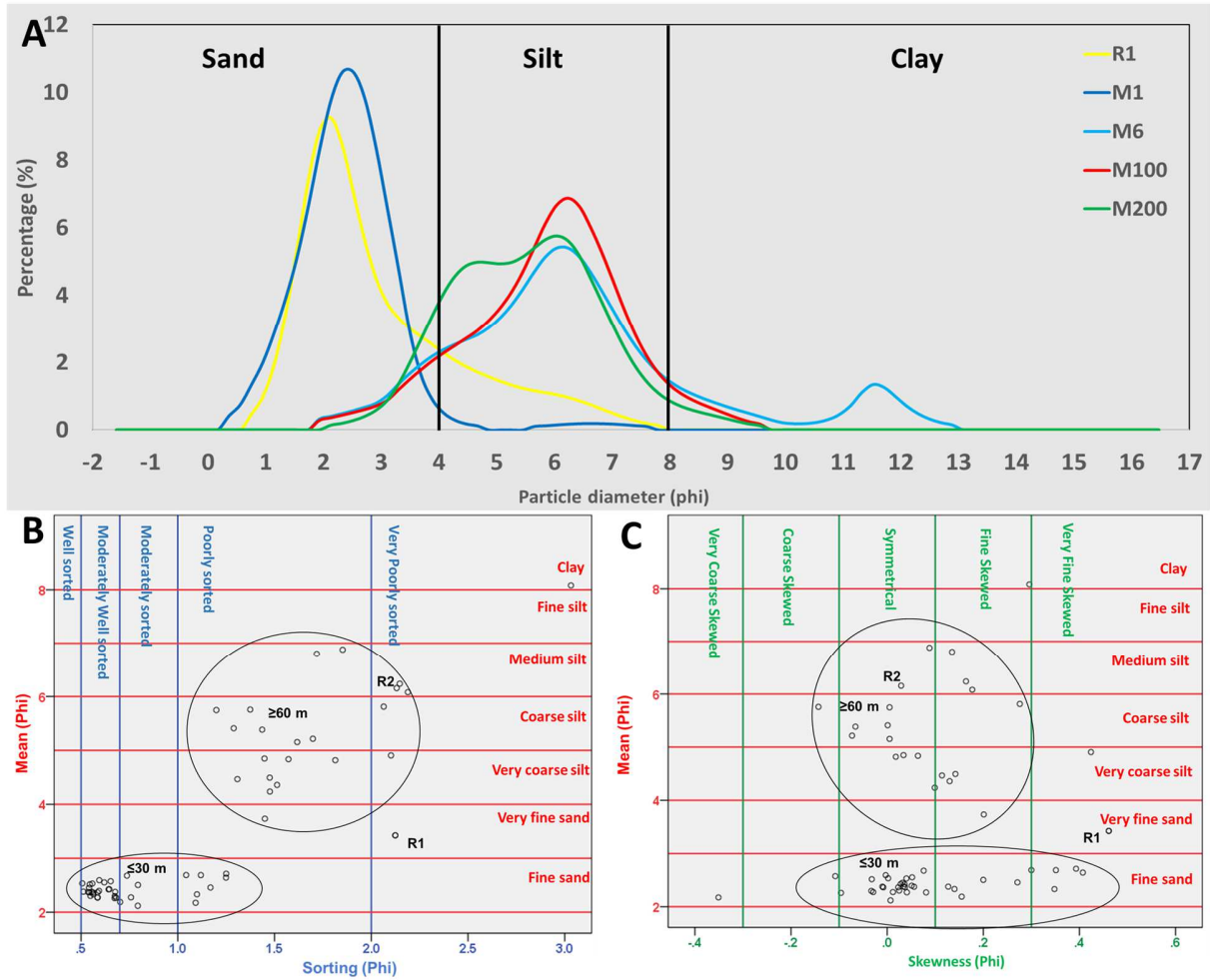
13 The CM plot (Figure 4 B) showed the occurrence of two different depositional conditions. Graded  
14 and uniform suspension without rolling characterized the deep stations ( $\geq 60$  m), while bottom  
15 suspension and rolling characterized the shallow stations ( $\leq 30$  m).

16 3.1.6. Linear Discriminant Analysis (LDA):

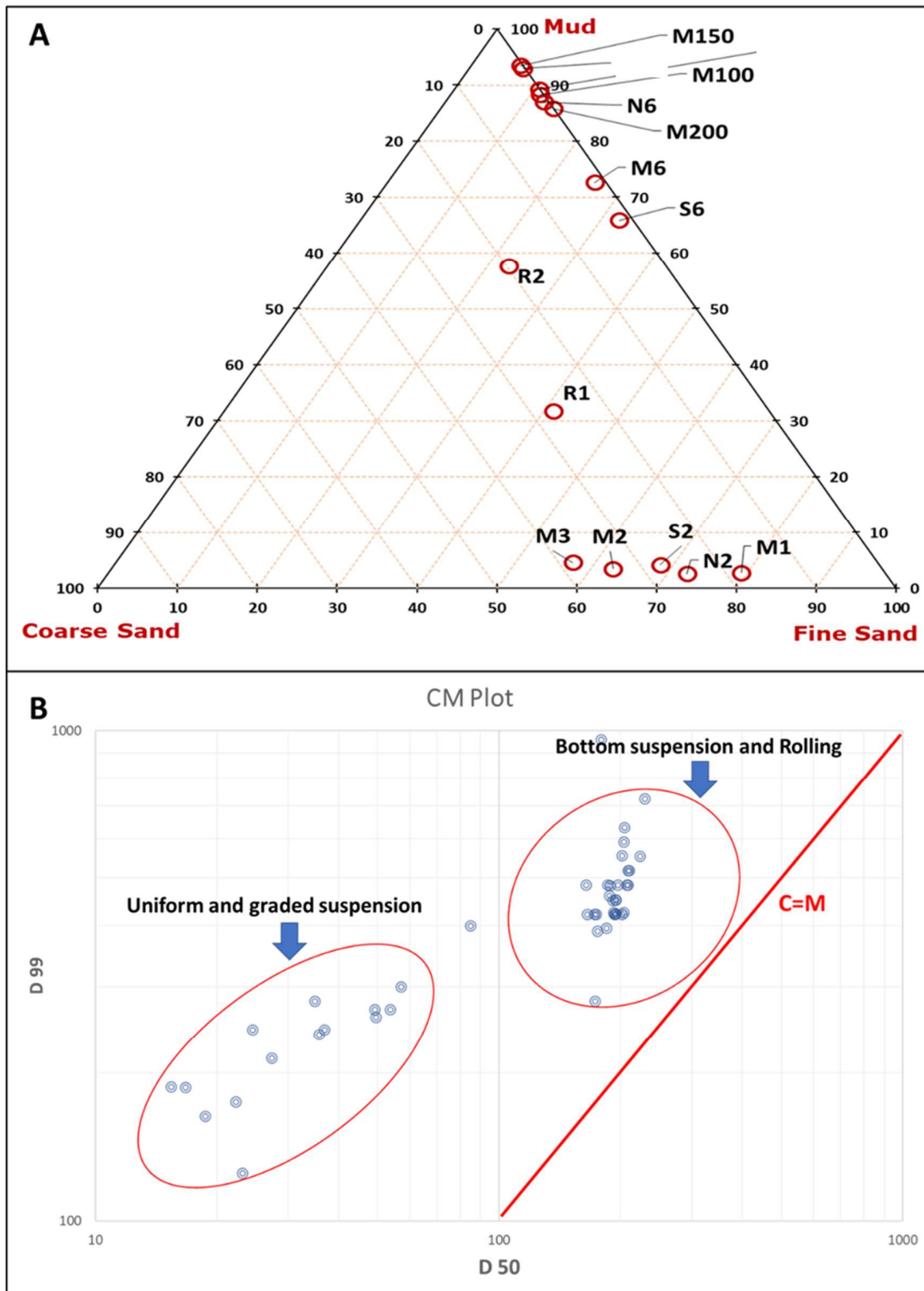
17 According to Y1 and Y2 respectively, most of the samples belonged to the shallow agitated water  
18 environment (Y1) and all the samples fell in the shallow marine condition (Y2) (Figure 5 A).

19 According to Y3, deep stations ( $\geq 60$  m) were characterized by fluvial processes, while shallow  
20 stations were characterized by a shallow marine process except for sampling dates: December  
21 2017 and April 2018 (Figure 5 A, B, C). According to Y4, the majority of the samples were  
22 attributed to turbidity current deposits in high hydrodynamic environments except for N6 in  
23 January 2017 and the sampling dates December 2017 and April 2018 that revealed high river

- 1 flow intensity recorded as fluvial process. These obtained results were verified by the river
- 2 samples which according to both Y3 and Y4, belong to a fluvial environment (Figure 5 B).

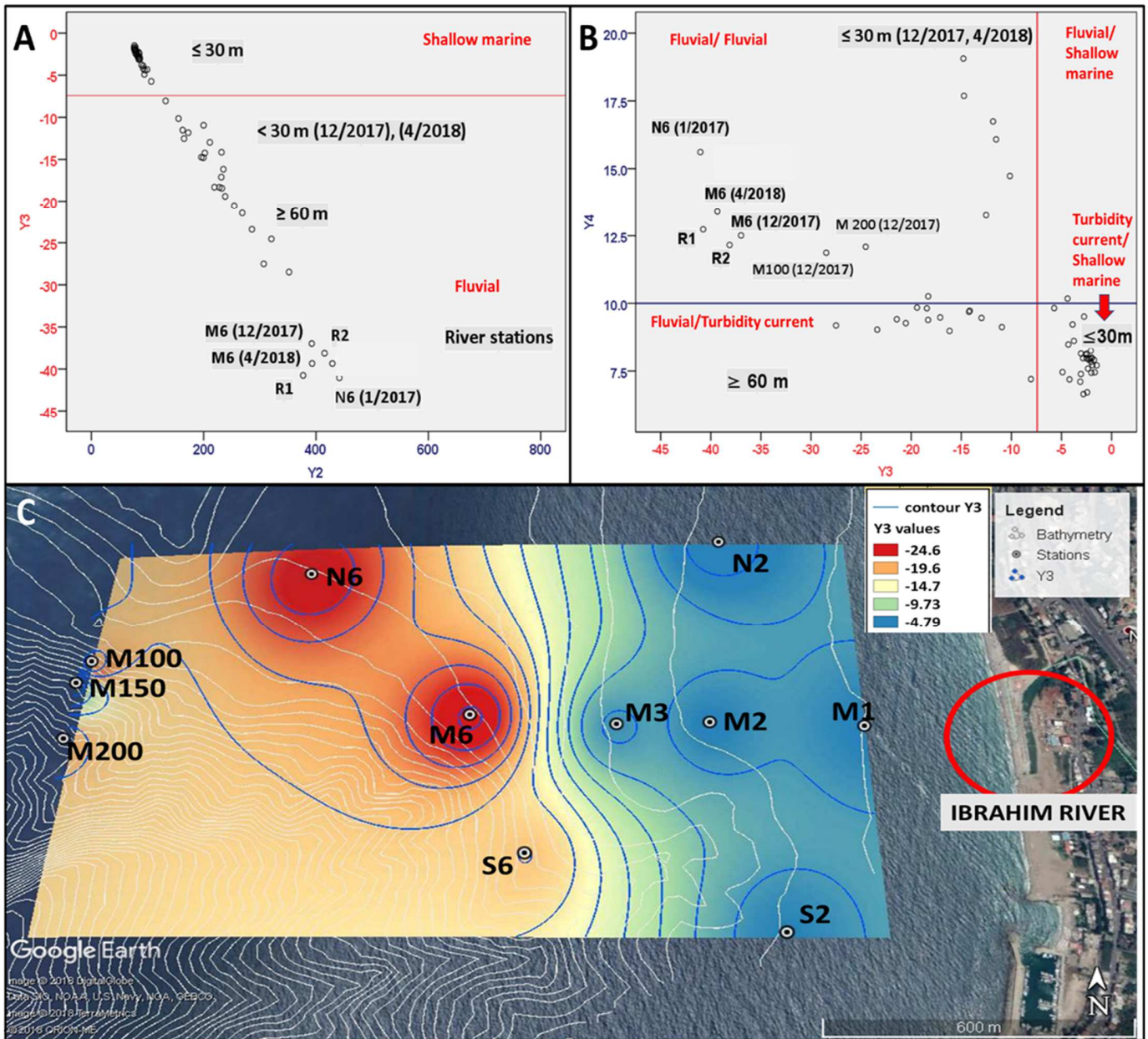


- 3
- 4 **Figure 3:** Grain size class weight distribution (A), Mean vs Sorting plot (B), Mean vs Skewness plot (C),
- 5 at the different sampling stations.



1

2 **Figure 4:** Ternary diagram representing the grain size distribution (A) and the C-M Plot (B) for the  
 3 sampling stations.



2 **Figure 5:** Linear Discriminate Function (LDF) Plots: Y3 vs Y2 plot (A), Y4 vs Y3 plot (B) and spatial  
 3 distribution of Y3 (C) at the studied area

4 **3.2. Organic carbon (OC) and total nitrogen (TN) distribution**

5 OC and TN contents (% dry weight) in the surface sediments of Ibrahim River coastal marine area  
 6 followed similar distributions, characterized by a strong regionality following the distribution of the  
 7 mud fraction (Figure 6). Low values occurred at shallow stations ( $\leq 30$  m) while high values

1 occurred at deep stations ( $\geq 60$  m). During almost all sampling dates, the lowest OC value of 0.1%  
2 occurred mainly at stations M1, M2 and M3 while the highest value, which is approximately 10  
3 times greater (1.19%), occurred at the deepest station of 200m (M200).

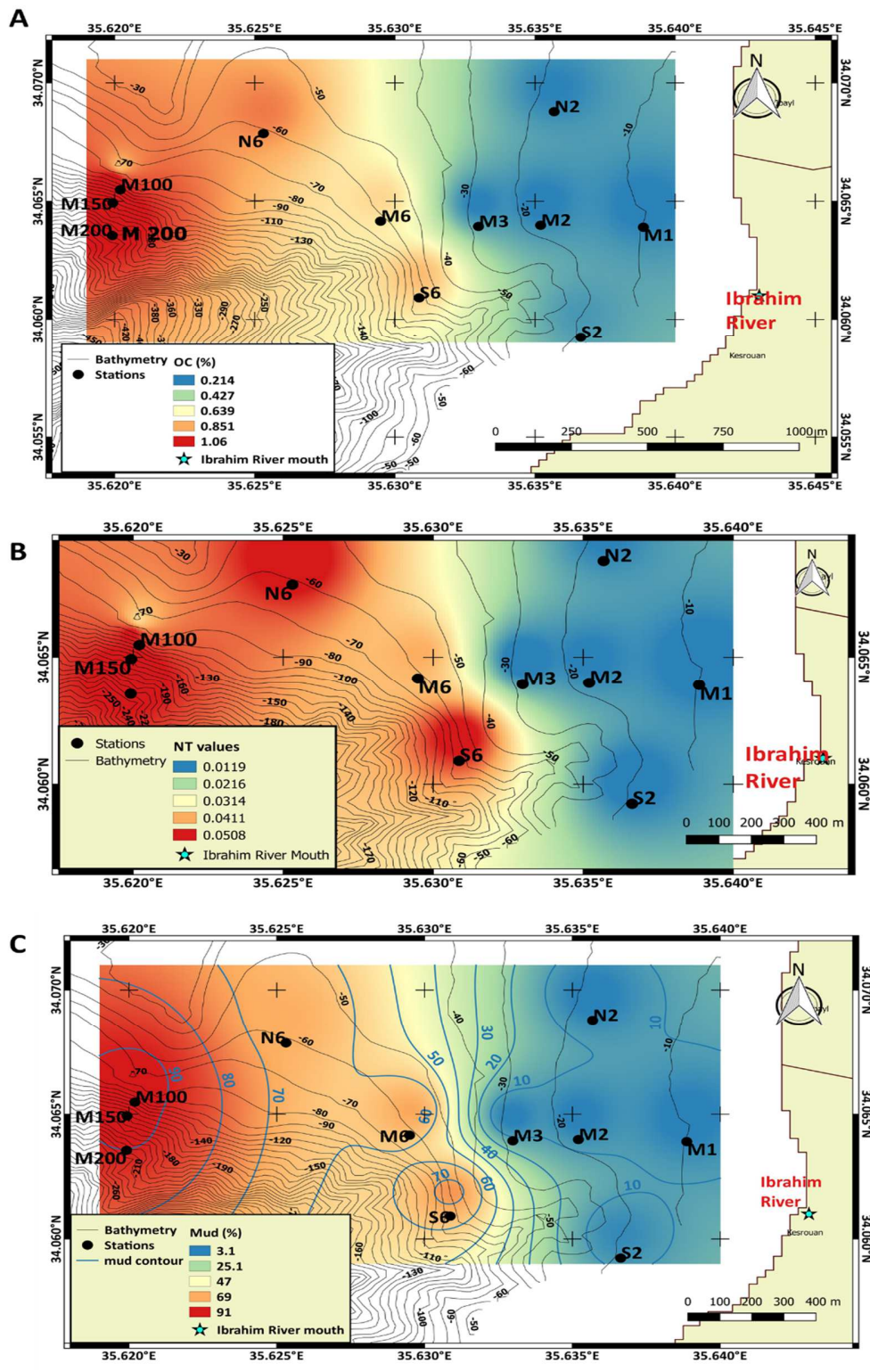
4 The lowest TN value (0.005%) was recorded at stations M1 and N2 while the highest TN (0.067%)  
5 occurred at station S6 in October 2016.

### 6 **3.3. Photosynthetic pigments and labile organic matter distributions**

7 Chlorophyll-a concentrations were very low and strongly decreasing with depth (Figure 7 A). The  
8 highest value of chlorophyll was recorded at station M2 in January 2017, reaching 1.54  $\mu\text{g/g}$  while  
9 nearly no values were detected at stations exceeding 100 m depth (M100, M150, M200). The  
10 phaeopigment concentrations varied from 0.06 to 4.85  $\mu\text{g/g}$  increasing with depth in opposition to  
11 chlorophyll. Concerning labile compounds (Table 3),  $\Sigma$  CHO, LPD, PRT as the sum of biochemical  
12 compounds (sugars, lipids and proteins) ranged from 0.525 to 2.671 mg/g. Lipids (0.298 to 1.683  
13 mg/g) were the dominant fraction followed by CHO (0.134 to 1.255 mg/g) and PRT (0.029 to 0.418  
14 mg/g), which were increasing with depth following the trend of fine fraction, OC, TN, and  
15 phaeopigments. Labile organic matter proportions (C-LOM/TOC%) (Figure 7 B) decreased with  
16 depth from 38% at the shallow stations ( $\leq 30$  m) to 10% recorded at the deep stations ( $\geq 60$  m).

17

18



1

**Figure 6:** Spatial distribution of organic carbon percentages OC (%) (A), total nitrogen percentages TN (%) (B) and mud fraction percentages (%) (C) at the studied area.

1

2 **Table 3:** Concentrations of geochemical and biochemical studied parameters in the sediments of the  
3 studied area

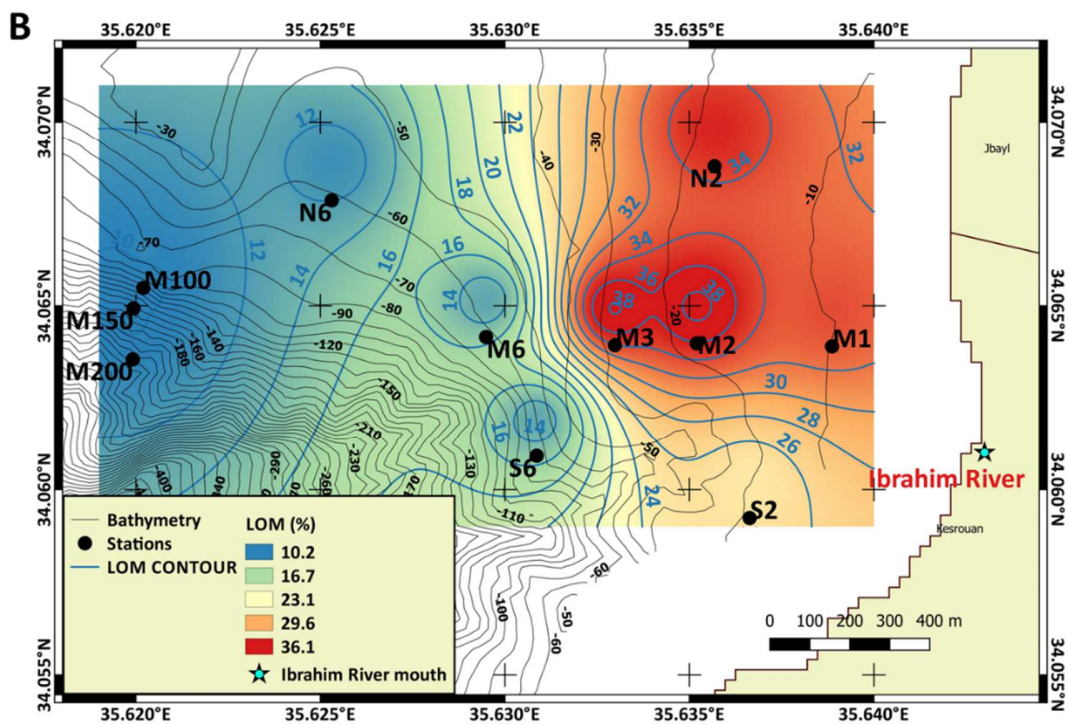
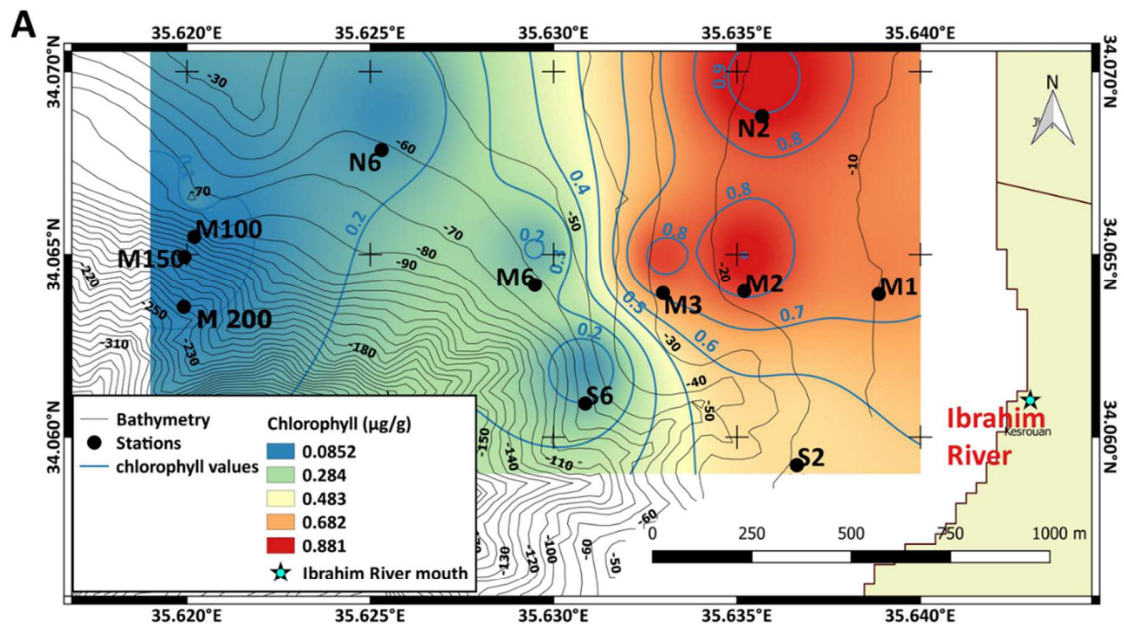
| Stations     | TN (%) | OC (%) | CHO (mg/g) | LPD (mg/g) | PRT (mg/g) | $\Sigma$ (CHO, LPD, PRT) | CLOM (mg/g) | CLOM/TOC % | PRT/CHO |
|--------------|--------|--------|------------|------------|------------|--------------------------|-------------|------------|---------|
| Min          | 0.005  | 0.1    | 0.134      | 0.298      | 0.029      | 0.525                    | 0.31        | 8          | 0.11    |
| Max          | 0.067  | 1.19   | 1.255      | 1.683      | 0.418      | 2.671                    | 1.533       | 87         | 0.59    |
| Mean         | 0.02   | 0.44   | 0.45       | 0.79       | 0.14       | 1.381                    | 0.8         | 27.63      | 0.30    |
| <b>RIVER</b> |        |        |            |            |            |                          |             |            |         |
| R1           | 0.03   | 0.54   | 0.92       | 0.62       | 0.18       | 1.72                     | 0.89        | 16.66      | 0.2     |
| R2           | 0.12   | 2.10   | 2.81       | 1.24       | 0.76       | 4.81                     | 2.36        | 11.24      | 0.27    |

4

#### 5 **3.4. $\delta^{13}\text{C}$ and terrestrial fraction distribution**

6  $\delta^{13}\text{C}$  values ranged from -21.63‰ to -25.27‰ (Figure 8 A). Low values occurred at the deep  
7 stations ( $\geq 60$  m). The least negative  $\delta^{13}\text{C}$  (-21.63‰) occurred at station M2 in July 2016, while  
8 the most negative value (-25.27‰) at station M6 in April 2018.

9



1

2 **Figure 7:** Chlorophyll spatial distribution (A) and labile organic matter percentages (LOM) spatial  
 3 distribution (B) at the studied area

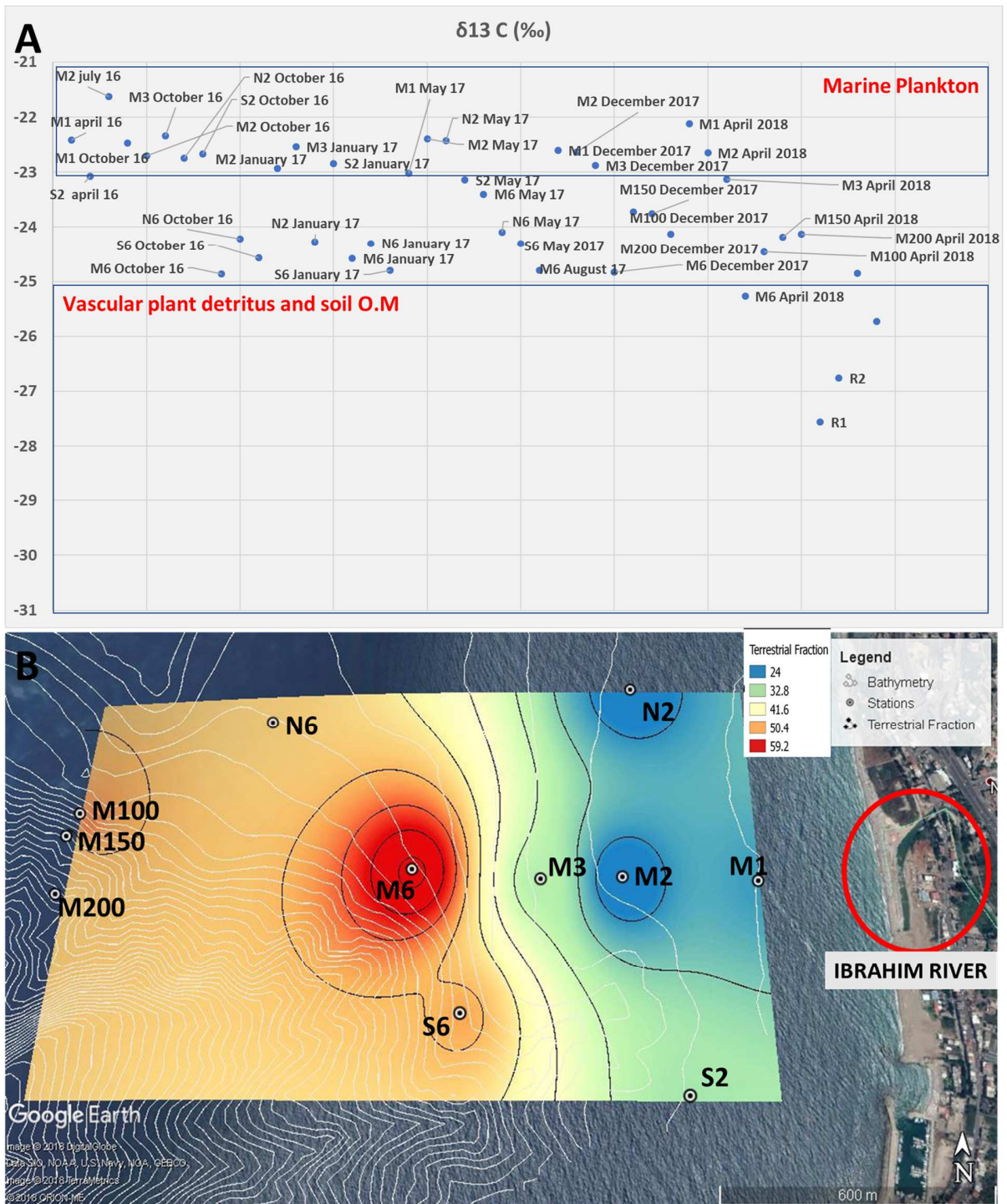


**Figure 8:**  $\delta^{13}C$  ranges and associated organic matter sources (A) and spatial distribution of the terrestrial fraction (B) at Ibrahim River coastal marine area

1 The terrestrial fraction percentages (Ft) in the studied area (Figure 8 B) varied between 9.7% at  
2 station M2 and 65.7% at station M6 in April 2018. Stations with Ft > 50% dominated by the  
3 terrestrial fraction were located off-shore in the depositional area ( $\geq 60$  m) and station N2 (North  
4 20m) in January 2017. Stations with Ft < 50% were located nearshore at stations  $\leq 30$  m.

## 5 **4. Discussion**

### 6 **4.1. Environment of depositions revealed by grain size analyses**

7 Continental shelves and specifically open ones usually act as bypass zones characterized by  
8 limited sediment supply and strong winnowing (Zhu et al., 2011).

9 Different types of grain sizes occurring at the studied area with a strong regionality may be the  
10 result of sorting due to geomorphology and hydrodynamics. These create different circulation  
11 modes associated with different sediment sources. At shallow stations ( $\leq 30$  m), sediments are  
12 exposed to wind and waves limiting the accumulation of clay-sized fractions. In fact, the deposition  
13 of coarser sediments takes place in high energy environments where resuspension may occur.  
14 Finer sediments are transported and deposited in sheltered windless environments, under low  
15 energy conditions, acting as depositional areas ( $\geq 60$  m) (Isla et al., 2006; Zhu et al., 2011 ;  
16 Manivel et al., 2016; Winogradow and Pempkowiak, 2018). Moreover, at the shallow stations ( $\leq 30$   
17 m), sediments are better sorted and dominated by coarser particles (fine sand), which reflect the  
18 occurrence of higher wave energy and strong hydrodynamics. Poorly sorted and finely to very  
19 finely skewed distribution characterizing sediments of the deepest stations ( $\geq 60$  m) indicate the  
20 addition of finer material from riverine input and the governance of low energy environments  
21 allowing the finer fraction to settle down (Manivel et al., 2016; Padhi et al., 2017).

22 Referring to Stokes's law, coarser particles settle faster than smaller ones. At the shallower  
23 sampling points, sediment mainly consists of coarser particles in relation with disturbed  
24 conditions: presence of waves and currents preventing the settlement of the finer fraction. At the

1 deeper sampling points, sediments are mainly constituted of finer fraction associated with calmer  
2 environments (McComb et al., 1998; Karageorgis et al., 2000). In general, sedimentation is  
3 affected by the different energetic and hydrodynamic conditions prevailing at the studied  
4 environment. The dominance of coarse size (here fine sand) denotes high energy conditions,  
5 whereas the dominance of the fine fraction (here silt) denotes low energy conditions (Amarjouf et  
6 al., 2014; Baiyegunhi et al., 2017; Padhi et al., 2017).

7 The case of Ibrahim River presents an originality to what is generally encountered in the rivers  
8 generating changes in the size characteristics of the coastal sediments; however, it is similar to  
9 the case encountered at the level of another Lebanese seasonal river "Al Jaouz" during a previous  
10 study by Fakhri et al., (2008). In fact, in addition to the river input characteristics which supply  
11 limited fine fraction due to the presence of the dam, the geomorphology of the coast plays a major  
12 role in the effect of the river input. The narrowness of the Lebanese continental shelf promotes  
13 the winnowing of the fine fraction offshore (Fakhri et al., 2018).

14 Sediment samples were moderately well sorted to very poorly sorted, thus, marking differences  
15 in the uniformity of particle size distribution between stations (Manivel et al., 2016). The negative  
16 skewness characterizing sediments of some shallow stations (M1, M2) reveals a loss of finer  
17 sediments in high energy environments. The near symmetrical distribution characterizing other  
18 shallow stations indicates the mixing of two particle populations generated from two different  
19 sources. Thus, the skewness values recorded are strongly affected by wave action prevailing in  
20 the studied area. Extremely high Kurtosis values occurring at station S2 and N6 in January 2017,  
21 as well as, stations M1, M2 and M3 in December 2017 and April 2018 indicates that part of the  
22 sediment is sorted elsewhere in high energy environments (Ramesh et al., 2015; Manivel et al.,  
23 2016; Padhi et al., 2017).

24 The combination of all grain size statistical parameters and plots may clearly differentiate between  
25 two types of sedimentary environments at the studied area: 1) Shallow stations ( $\leq 30$  m) dominated

1 by fine sand (coarsest particles) and characterized by the best sorting and a symmetrical  
2 distribution transported by rolling and suspension in high energy shallow agitated marine water;  
3 2) Deep stations ( $\geq 60$  m) dominated by silt (finest particles) and characterized by positive  
4 skewness and poorly sorted sediments that are transported by uniform graded suspension,  
5 settled in low energy environment and considered as fluvial deposits (Kulkarni et al., 2015).

#### 6 **4.2. OC, TN, LOM and photosynthetic pigments spatial distribution**

7 The obtained amounts of OC and TN are associated with each grain size fraction and affected by  
8 the hydrodynamic sorting of grain size distribution.

9 The obtained results are similar to those recorded in front of the Tet coastal river in the north-  
10 western basin of the Mediterranean, with annual averages of 0.2% in littoral sands (at 20 m depth)  
11 and 0.55%(28 m) in silts and 0.95% in the central mudflat of the continental shelf (at 60-80 m  
12 depth) (Pruski et al., 2019). The recorded values may also be compared to those obtained at the  
13 east China Sea shelf system facing the Yangtze River, representing low OC (0.1 to 1.3%) and TN  
14 (0.005% to 0.14%) values while OC values of (0.1 to 4%) are found in other continental margins  
15 reaching 5.9% at the Baltic Sea (Zhu et al., 2011; Winogradow and Pempkowiak, 2018).

16 OC and TN are significantly correlated with the mud fraction of sediments ( $r=0.92$ ,  $p<0.001$ ,  $K=36$   
17 and  $r=0.85$ ,  $p<0.001$ ,  $K=36$  respectively) suggesting that the fine fraction (Silt-Clay) is the primary  
18 controlling factor of the organic matter concentration in sediments of the studied area.

19 In fact, the preservation of organic matter is strongly affected by the presence of fine fraction  
20 characterized by greater surface area allowing the sorption of organic matter into the clay particles  
21 and the aggregation with silt fraction. Furthermore, the strong correlation existing between OC  
22 and TN ( $r=0.94$ ,  $p<0.001$ ,  $K=36$ ) may suggest that they share the same origin and that the majority  
23 of nitrogen is from organic one (Sondi et al., 2008; Zhu et al., 2011; Li et al., 2016; Abballe and  
24 Chivas, 2017; Quiros-Collazos et al., 2017).

1 Carbohydrate values (0.134-1.255 mg/g) were slightly lower than those recorded by Pusceddu et  
2 al. (1999) in the sediments of the eastern and western basins of the Mediterranean Sea (1.2-2.4  
3 mg/g and 0.9-4.2 mg/g respectively). High concentrations were recorded at 60 m depth in  
4 association with high organic carbon concentrations and low photosynthetic pigments. Those  
5 results witness the effect of hydrodynamics that governs the coastal zone such as waves, currents  
6 and river flow carrying the particles offshore. Moreover, those high concentrations remaining at  
7 deep levels may result from the terrestrial origin of carbohydrates. In fact, terrestrial sugars are  
8 highly refractive (such as cellulose) while planktonic marine sugars are mainly hydrolysable  
9 particles (Fabiano and Pusceddu, 1998).

10 Lipid concentrations (0.298 - 1.683 mg/g) were higher than those recorded in the sediments of  
11 the western (0.01-0,66 mg/g) and eastern Mediterranean Sea (0.05-0.19 mg/g) (Fabiano and  
12 Pusceddu, 1998), and in the Ligurian Sea (0.02-0.21) (Fabiano et al., 1995; Cividanes et al.,  
13 2002). Higher concentrations of lipids are associated with photosynthetic pigment concentrations.  
14 Lipids may originate from the decay of plankton, since it is a major constituent of cell membranes.  
15 Moreover, high lipid concentrations may also result from the terrestrial and river inputs, as well  
16 as, anthropogenic activities in the adjacent land.

17 The concentrations of proteins (0.03 - 0.42 mg/g) were close to those found in the oligotrophic  
18 basin of the Ligurian Sea (0.02 - 0.07 mg/g) (Fabiano et al., 1995; Cividanes et al., 2002). The  
19 obtained values are considered low when compared to the values recorded at the western  
20 Mediterranean Sea (0.5 - 2.6 mg/g) and the Baltic Sea (3.8 - 7.7 mg/g) considered as highly  
21 productive basins (Pusceddu et al., 1999; Cividanes et al., 2002).

22 High levels of proteins associated with high organic matter concentrations and finer fraction were  
23 measured at deep stations. Shallow sampling points contain less proteins due to active  
24 hydrodynamic conditions (Fabiano and Pusceddu, 1998).

1 The mean value of LOM proportion (28% of TOC) is close to those found at highly oligotrophic  
2 sites (20% of TOC), and higher than those found at eutrophic ecosystems (3%). Despite the high  
3 concentrations of total organic matter at eutrophic sites, the labile fraction increases when  
4 proceeding from eutrophic to oligotrophic sites with an increase in food quality (Fabiano et al.,  
5 1995).

6 The continental shelf in Lebanon is very narrow; there are no closed bays and water is  
7 permanently mixed leading to a fast dispersion of nutrients and pollutants.

8 Moreover, even the stations facing river estuaries in Lebanon are not characterized by high  
9 concentrations of chlorophyll, which is probably due to the high prevailing turbidity conditions  
10 (instability) and low concentrations of orthophosphates (essential element for the primary  
11 production) (Abboud-Abi Saab et al., 2008).

#### 12 **4.3. Seasonal variations of granulometric, geochemical and biochemical parameters**

13 At deep stations ( $\geq 60$  m), seasonal variation was significant for the following parameters: mean  
14 grain size, protein, CLOM/TOC, lipids, total nitrogen. For mean grain size, a significant difference  
15 existed between dry season (August) and wet season (December, January and April) (p-value:  
16 0.015). During the wet season, the highest values were recorded, indicating the addition of fine  
17 sediments by fluvial inputs. On the other hand, for proteins, CLOM/TOC, lipids and total nitrogen,  
18 the highest values were recorded in the dry season (August and October) showing a significant  
19 difference with the wet season (December, January and April). This difference can be attributed  
20 to the increase in fluvial inflow during the wet season resulting in a dilution of the labile  
21 compounds.

22 At the littoral stations ( $\leq 30$  m), the seasonal difference is significant for the following parameters:  
23 mean grain size, sorting, Y3 and Y4, organic carbon, carbohydrates, lipids, labile organic matter  
24 (CLOM / TOC), chlorophyll-a and phaeopigments.

1 For granulometric parameters, a significant difference exists between December and April  
2 representative of the wet season and May, June, July, October representative of the dry season.  
3 The wet season is characterized by higher values of mean grain size and sorting illustrating the  
4 addition of fine sediment by fluvial input, as well as, more negative values of Y3 and Y4, reporting  
5 the river environment.

6 For organic carbon and carbohydrates, the wet season (December and January) is characterized  
7 by low values. These compounds were probably transferred with the fine fraction at deep stations.

8 On the other hand, chlorophyll, labile organic matter (CLOM/TOC) and lipids follow almost the  
9 same seasonal distributions with the highest values occurring in January 2017.

10 The highest concentrations of phaeopigments are recorded in June when chlorophyll values are  
11 minimal, after the spring bloom, while the lowest values of phaeopigments are recorded for the  
12 months of October, January and December.

13 The highest chlorophyll-*a* concentrations representing the microphytobenthic biomass in the  
14 sediments of the studied area were reported in January, July, October and December, while the  
15 phytoplankton bloom in Lebanese waters occurs during spring and early summer (June–August)  
16 (Abi Saab et al., 2008; Lakkis, 2018). The settlement of photosynthetic cells usually occurs during  
17 the first week following the bloom and then, phytoplankton abundance may be insignificant  
18 (Fabiano et al., 1995). It is important to mention the opposite trend between the temporal variation  
19 of the photosynthetic pigment concentrations in surface sediments (maximum in winter) and in  
20 water (maximum in summer), this situation is also reported by Magni and Montani (2006).

21 Moreover, seasonal variation in the concentrations of photosynthetic pigments is probably  
22 affecting the content of labile organic matter in sediments, thus, estimating the effective amount  
23 of the bioavailable fraction (Fabiano et al., 1995).

24

#### 25 **4.4. PRT:CHO ratio and trophic status**

1 The PRT: CHO ratio is used to determine the degradation state of organic material in an aquatic  
2 ecosystem. In fact, proteins are used more by bacterial organisms than carbohydrates. A low  
3 PRT: CHO ratio indicates degraded organic matter while a high ratio indicates new deposited  
4 organic material. Usually the dominance of the carbohydrates fraction in the labile organic fraction  
5 is considered as an indicator of oligotrophic conditions (Pusceddu et al., 1999).

6 The PRT: CHO ratio (0.11-0.59) appears to be lower than 1 in the sediment of all sampling points.  
7 This situation indicates the dominance of degraded material, as well as, the occurrence of  
8 terrestrial material. The dominance of carbohydrates over proteins may also indicate a refractory  
9 nature of organic matter, associated with high detritus referring to allochthonous and heterotrophic  
10 material carried by the river. The ratios found are close to those found in the Ligurian Sea (0.14)  
11 and the eastern Mediterranean Sea (0.09), considered as oligotrophic sites, and lower than the  
12 values occurring at the Arno estuary (Australia) (0.3-3.6) (Fabiano et al., 1995; Cividanes et al.,  
13 2002).

14 The benthic trophic classification may be identified according to the PRT: CHO ratio and labile  
15 organic matter concentrations. The sum of labile compounds ( $\Sigma$ CHO, LPD,PRT) ranging from  
16 0.525 to 2.671 mg/g is almost similar to the value measured by Fakhri et al., (2008) in the northern  
17 Lebanese coastal marine area (0.5-2.5 mg/g). The values of labile compounds represented as C  
18 equivalents (CLOM :0.31 to 1.533 mg/g) indicate the prevalence of a meso-oligotrophic status  
19 (Pusceddu et al., 2011). Moreover, the PRT concentration is between 0.03 mg/g and 0.42 mg/g,  
20 the CHO concentration is between 0.13 mg/g and 1.26 mg/g, and the PRT: CHO ratio is less than  
21 1. Therefore, the benthic ecosystem may be considered as meso-oligotrophic to oligotrophic  
22 (Dell'Anno et al., 2002).

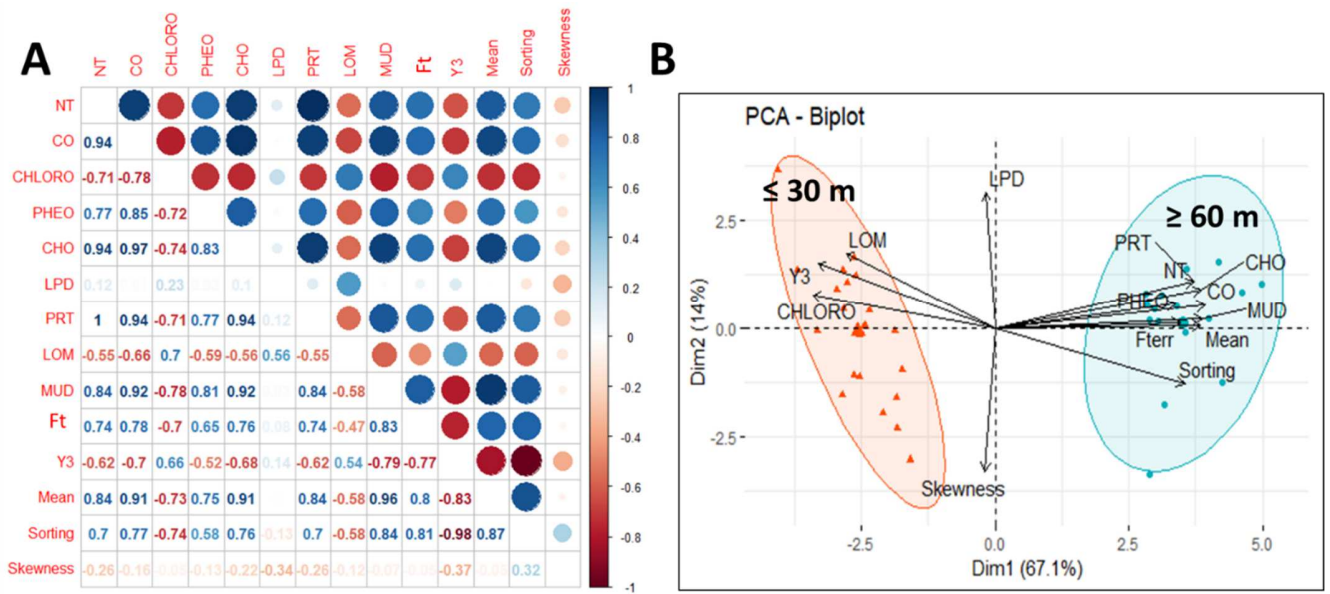
#### 23 **4.5. Source and degradation degree of the organic matter**

1 Mixed sources of organic matter are revealed by the  $\delta^{13}\text{C}$  values. The obtained  $\delta^{13}\text{C}$  values are  
2 similar to the values recorded at the Yangtze river estuary (-24.5‰ to -21.2‰) but less negative  
3 than the values published in the Colville River estuary (-27.1‰ to -25‰) and facing the Amazon  
4 River (-24‰ to -27‰) (Li et al., 2016).

5 The two primary origins of organic matter in the studied area may be terrestrial, which is mainly  
6 due to the Ibrahim River input, and coastal marine autochthonous.  $\delta^{13}\text{C}$  ranges discriminate  
7 between marine organic matter from planktonic origin (-21.6‰) in shallow stations ( $\leq 30$  m) and  
8 the mixture between terrestrial and marine particles with a dominance of the terrestrial fraction  
9 (soil organic matter and vascular plants debris) reaching the deep stations ( $\geq 60$  m) (-23 and -  
10 25‰). This reveals a significant input of terrestrial organic carbon transported mainly by the river  
11 reaching deep stations and indicates a decrease of planktonic labile fresh organic matter  
12 contribution (Li et al., 2016; Abballe and Chivas, 2017; Winogradow and Pempkowiak, 2018).

13 High percentages of allochthonous terrestrial fraction were recorded at the sheltered depositional  
14 areas ( $\geq 60$  m) while the shallow exposed areas ( $\leq 30$  m) (strong hydrodynamics) showed low  
15 percentage of terrestrial organic matter (Incera et al., 2003).

16 The two variables LOM and Ft are inversely correlated ( $r=-0.47$ ,  $p<0.01$ ,  $K=36$ ) (Figure 9 A). The  
17 fact that the lability of organic matter decreases with the increase of the terrestrial fraction  
18 indicates that fresh labile organic matter originates mainly from marine planktonic origin. High  
19 LOM percentages reaching 70% generally occur in shallow nearshore areas (Isla et al., 2006;  
20 Wang et al., 2018).



1

2

**Figure 9:** Organic composition and grain size distribution in surface sediments: Correlation Matrix (N=38 K=36  $r=0.324$ ,  $p<0.05$ ;  $r=0.418$ ,  $p<0.01$ ;  $r=0.518$ ,  $p<0.001$ ) (A)

PCA Biplot: Two components exhibiting 81.1% of the total variance F1 (67.1%) and F2 (14%) distinguishing two groups of parameters associated with two groups of stations according to F1 (B)

1 A strong correlation was recorded between chlorophyll and food indicators (LOM) ( $r=0.7$ ,  $p<0.001$ ,  
 2  $K=36$ ). In fact, high concentrations of labile organic matter and chlorophyll was recorded at the  
 3 shallower stations (Figure 9 B). This fact may refer to the dominance of the autochthonous marine  
 4 material issued from the primary production at the shallower stations, as shown by  $\delta^{13}C$  values  
 5 and the percentage of terrestrial fraction. This is contrary to the case of the Adriatic Sea, facing  
 6 the Po River, where chlorophyll concentrations in sediment, affected by the river plume, increased  
 7 from 0.8 to 1.6  $\mu\text{g/g}$  when proceeding off-shore due to the light obstruction of river suspended  
 8 particles (Dell'Anno et al., 2008; Liu et al., 2015).

1 Moreover, the difference in grain size distribution among the stations seems to affect the  
2 distribution and the degree of degradation of organic matter (Wang et al., 2018). The mud  
3 dominated area ( $\geq 60$  m) characterized by silt-clay fraction is associated with a high OC value and  
4 a low LOM content. This is reflected through the strong positive correlation occurring between  
5 mud and OC ( $r=0.92$ ,  $p<0.001$ ,  $K=36$ ) and TN ( $r=0.84$ ,  $p<0.001$ ,  $K=36$ ), respectively. This is in  
6 opposition to the strong negative correlation between mud and LOM ( $r=-0.55$ ,  $p<0.001$ ,  $K=36$ ).

7 A preservation phenomenon of organic matter in sediments was marked from shallow ( $\leq 30$  m) to  
8 deep stations ( $\geq 60$  m) where the refractory organic matter fraction (biochemically resistant)  
9 becomes dominant. At these depositional areas, the labile fraction decreases in association with  
10 the decrease of the marine planktonic autochthonous contribution and the increase of the  
11 terrestrial fraction. Terrestrial organic matter accumulating in marine ecosystems is mainly  
12 composed of refractory organic matter while marine autochthonous organic matter from plankton  
13 origin is mainly labile and directly mineralized. Higher percentages of refractory organic matter  
14 are mainly due to the loss by mineralization of the labile organic matter during the transport of  
15 organic matter from near shore (higher energy conditions) to the deepest depositional areas  
16 (Winogradow and Pempkowiak, 2018).

17 The terrestrial fraction deducted from  $\delta^{13}\text{C}$  ratio of organic matter differentiates between two types  
18 of environments ( $\leq 30$  m and  $\geq 60$  m) associated with two depositional environments revealed by  
19 grain size analyses (Figure 9 B) and verified by the Kruskal Wallis and Dunn test ( $p$  value  $<0.05$   
20 for all the variables).

## 21 **5. Conclusion**

22 The actual research work demonstrates that a combination of both granulometric and organic  
23 matter parameters including the carbon isotopic ratio ( $\delta^{13}\text{C}$ ) is able to differentiate between the  
24 sources of sediments and its associated organic matter among marine and terrestrial origins using

1 sediment samples collected from the Ibrahim River watershed and its adjacent coastal marine  
2 area.

3 The studied area is found to be characterized by two depositional environments associated with  
4 two different sources of organic matter, respectively. The high energy nearshore shallow marine  
5 area ( $\leq 30$  m) is characterized by sediments that are dominated by fine sand and characterized  
6 by low values of organic carbon and total nitrogen. At these sampling points, organic matter is  
7 mainly fresh and from marine autochthonous source witnessed by the occurrence of higher LOM  
8 percentages and chlorophyll-*a* concentrations. The deep windless low energy marine area ( $\geq 60$   
9 m) is characterized by sediments that are dominated by the fine fraction considered as fluvial  
10 deposits carried by the Ibrahim River flow and characterized by high OC and TN values. At these  
11 sampling points, the organic matter fraction is mainly refractory and from terrestrial allochthonous  
12 origin as revealed by the  $\delta^{13}\text{C}$  values.

13 Moreover, according to the PRT:CHO ratio and the concentration of labile organic matter, the  
14 benthic ecosystem could be considered as meso-oligotrophic to oligotrophic.

15 This study provides an accurate estimation of organic matter origin (marine or terrestrial) and  
16 presents a new valuable sediment tracing tool by combining grain size composition of sediments  
17 with the carbon isotopic signature ( $\delta^{13}\text{C}$ ) of its associated organic matter. In addition, it is  
18 considered as an innovative research work for the coastal eastern Mediterranean Basin, and it  
19 could establish a starting point of comparison with numerous other studies conducted along the  
20 coastal western Basin.

## 21 **Acknowledgments**

22 This paper constitutes a part of the PhD of Myriam Ghsoub, supported by the CNRS-L (National  
23 Council for Scientific Research-Lebanon) scholarship. The authors would like to thank the  
24 NCMS/CNRS-L (National Center for Marine Sciences) and the CEFREM (Centre de Formation

1 et de Recherche sur les Environnements Méditerranéens UMR 5110 (CNRS France) Université  
2 de Perpignan - Via Domitia for hosting this work and providing technical assistance. The authors  
3 would also like to thank the Platform for Research and Analysis in Environmental Sciences of the  
4 Lebanese University (UL) for grain size analysis.

## 5 **BIBLIOGRAPHY**

- 6 Abballe, P.A., Chivas, A.R., 2017. Organic matter sources, transport, degradation and preservation on a narrow rifted continental  
7 margin: Shoalhaven, southeast Australia. *Org. Geochem.* 112, 75–92. <https://doi.org/10.1016/j.orggeochem.2017.07.001>
- 8 Abboud-Abi Saab, M., 1985. Contribution à l'étude des populations microplanctoniques des eaux côtières libanaises (Méditerranée  
9 Orientale). Université d'Aix-Marseille II.
- 10 Abboud-Abi Saab, M., Fakhri, M., Kassab, M.-T., Matar, N., 2012. Spatial and vertical influence of river inputs on the marine primary  
11 production in Lebanese coastal waters : A case study, in: INOC-CNRS, International Conference on "Land-Sea Interactions in  
12 the Coastal Zone." Jounieh-Lebanon, pp. 62–73.
- 13 Abboud-Abi Saab, M., Fakhri, M., Sadek, E., Matar, N., 2008. An Estimate of the Environmental Status of Lebanese Littoral Waters  
14 Using Nutrients and Chlorophyll-A as Indicators. *Leban. Sci. J.* 9, 43–60.
- 15 Abuodha, J.O.Z., 2003. Grain size distribution and composition of modern dune and beach sediments, Malindi Bay coast, Kenya. *J.*  
16 *African Earth Sci.* 36, 41–54. [https://doi.org/10.1016/S0899-5362\(03\)00016-2](https://doi.org/10.1016/S0899-5362(03)00016-2)
- 17 Amarjoun, N., Hammadi, A., Oujidi, M., Rezqi, H., 2014. Sedimentological, geochemical and morphoscopic characterization of  
18 sediments from Nador Harbor (Morocco). *Bull. l'institut Sci. Rabat, Sect. Sci. la Terre* 36, 1–11.
- 19 Assaker, A., 2016. Hydrologie et Biogéochimie du Bassin Versant du Fleuve Ibrahim : Un Observatoire du Fonctionnement de la  
20 Zone Critique au Liban. Institut National Polytechnique de Toulouse (INP Toulouse).
- 21 Baiyegunhi, C., Liu, K., Gwavava, O., 2017. Grain size statistics and depositional pattern of the Ecca Group sandstones, Karoo  
22 Supergroup in the Eastern Cape Province, South Africa. *Open Geosci.* 9, 554–576. <https://doi.org/10.1515/geo-2017-0042>
- 23 Barnes, H., Blackstock, J., 1973. Estimation of lipids in marine animals and tissues: detailed investigation of the  
24 sulphophosphovanillin method for 'total' lipids. *J. Exp. Mar. Bio. Ecol.* 12, 103–118.
- 25 Besse, P.C., 1992. PCA stability and choice of dimensionality. *Stat. Probab. Lett.* 13, 405–410.
- 26 Blott, S.J., Pye, K., 2001. Gradistat: A grain size distribution and statistics package for the analysis of unconsolidated sediments.  
27 *Earth Surf. Process. Landforms* 26, 1237–1248. <https://doi.org/10.1002/esp.261>
- 28 Brink, R., Dubach, P., Lynch, D., 1960. Measurement of Carbohydrates in soil hydrolyzates with Anthrone. *Soil Sci.* 89, 157–166.
- 29 Cividanes, S., Incera, M., Lopez, J., 2002. Temporal variability in the biochemical composition of sedimentary organic matter in an  
30 intertidal flat of the Galician coast (NW Spain). *Oceanol. Acta* 25, 1–12.
- 31 Dell'Anno, A., Mei, M.L., Pusceddu, A., Danovaro, R., 2002. Assessing the trophic state and eutrophication of coastal marine  
32 systems: A new approach based on the biochemical composition of sediment organic matter. *Mar. Pollut. Bull.* 44, 611–622.  
33 [https://doi.org/10.1016/S0025-326X\(01\)00302-2](https://doi.org/10.1016/S0025-326X(01)00302-2)
- 34 Dell'Anno, A., Pusceddu, A., Langone, L., Danovaro, R., 2008. Biochemical composition and early diagenesis of organic matter in  
35 coastal sediments of the NW Adriatic Sea influenced by riverine inputs. *Chem. Ecol.* 24, 75–85.  
36 <https://doi.org/10.1080/02757540701814580>
- 37 El Najjar, P., Kassouf, A., Probst, A., Probst, J.L., Ouaini, N., Daou, C., El Azzi, D., 2019. High-frequency monitoring of surface  
38 water quality at the outlet of the Ibrahim River (Lebanon): A multivariate assessment. *Ecol. Indic.* 104, 13–23.  
39 <https://doi.org/10.1016/j.ecolind.2019.04.061>
- 40 Elias, A., 2006. Le chevauchement de Tripoli-Saida: croissance du Mont-Liban et risque sismique. Institut de Physique du Globe de  
41 Paris.
- 42 Emery, K.O., Heezen, B.C., Allan, T.O., 1966. Bathymetry of the Eastern Mediterranean sea. *Deep Sea Res.* 13, 173–192.
- 43 Fabiano, M., Danovaro, R., 1994. Composition of organic matter in sediments facing a river estuary (Tyrrhenian Sea): relationships  
44 with bacteria and microphytobenthic biomass. *Hydrobiologia* 277, 71–84.

- 1 Fabiano, M., Danovaro, R., Frascchetti, S., 1995. A three-year time series of elemental and biochemical composition of organic  
2 matter in subtidal sandy sediments of the Ligurian Sea (northwestern Mediterranean). *Cont. Shelf Res.* 15, 1453–1469.  
3 [https://doi.org/10.1016/0278-4343\(94\)00088-5](https://doi.org/10.1016/0278-4343(94)00088-5)
- 4 Fabiano, M., Pusceddu, A., 1998. Total and hydrolysable particulate organic matter (Carbohydrates, proteins, lipids) at a coastal  
5 station in Terra Nova Bay (Ross Sea, Antarctica). *Polar Biol* 19, 125–132.
- 6 Fakhri, M., Abboud-Abi Saab, M., Romano, J., 2008a. The use of sediments to assess the impact of Selaata Phosphate Plant on  
7 Batroun Coastal area ( Lebanon , Levantine Basin ). *Leban. Sci. J.* 9, 29–42.
- 8 Fakhri, M., Abboud-Abi Saab, M., Romano, J., Mouawad, R., 2008b. Impact of phosphate factory on the biological characteristics of  
9 North Lebanon surface sediments ( Levantine Basin ) [WWW Document]. <hal-00357034>.
- 10 Fakhri, M., Ghanem, A., Ghsoub, M., Ghaith, A., 2018. Environmental status of the bay of Jounieh through the evaluation of its  
11 marine sediments' characteristics. *Leban. Sci. J.* 19, 418–433.
- 12 Fitzpatrick, A., Fox, J., Leung, K., 2001. Environmental Baseline Survey of the Nahr Ibrahim, Lebanon. Massachusetts Institute of  
13 Technology, Cambridge.
- 14 Folk, R.L., Ward, W.C., 1957. Brazos River Bar: A Study in the significance of grain size parameters. *J. Sediment. Petrol.* 27, 3–26.
- 15 Goedicke, T.R., 1973. Distribution of surface currents and drift along the central continental shelf of Lebanon as related to pollution.  
16 Beyrouth.
- 17 Grenier, J.-F., 2014. Caractérisation pétrographique et pétrophysique du groupe de postdam dans le forage A203, Basses-Terres  
18 du Saint Laurent. Québec.
- 19 Higuera, M., 2014. Impact of eastern storm on the transfer of particulate organic matter into the Gulf of Lion (NW Mediterranean  
20 Sea). Université de Perpignan Via-Domitia.
- 21 Incera, M., Cividanes, S.P., Lastra, M., López, J., 2003. Temporal and spatial variability of sedimentary organic matter in sandy  
22 beaches on the northwest coast of the Iberian Peninsula. *Estuar. Coast. Shelf Sci.* 58, 55–61. [https://doi.org/10.1016/S0272-7714\(03\)00040-4](https://doi.org/10.1016/S0272-7714(03)00040-4)
- 24 Isla, E., Rossi, S., Palanques, A., Gili, J.M., Gerdes, D., Arntz, W., 2006. Biochemical composition of marine sediment from the  
25 eastern Weddell Sea (Antarctica): High nutritive value in a high benthic-biomass environment. *J. Mar. Syst.* 60, 255–267.  
26 <https://doi.org/10.1016/j.jmarsys.2006.01.006>
- 27 Karageorgis, A., Anagnostou, C., Sioulas, A., Eleftheriadis, G., Tsirambides, A., 2000. Distribution of surficial sediments in the  
28 Southern Evoikos and Petalioi Gulfs, Greece. *Mediterr. Mar. Sci.* 1, 111–122.  
29 <https://doi.org/http://dx.doi.org/10.12681/mms.282>
- 30 Khalaf, G., 1984. Contribution à l'étude écologique des fleuves côtiers du Liban : 2- cours moyen et inférieur du Nahr Ibrahim. *Bull.*  
31 *Mens. la Société Linnéenne Lyon* 53, 9–20.
- 32 Khalaf, G., Slim, K., Abi Ghanem, C., Nakhlé, K., Fakhri, M., 2009. Caractérisation et corrélation des paramètres biotiques et  
33 abiotiques des eaux du Nahr El Bared. *Leban. Sci. J.* 10, 3–21.
- 34 Khalaf, G., Slim, K., Saad, Z., Nakhlé, K.F., 2007. Evaluation de la qualité biologique des eaux du Nahr el Jaouz (Liban) : application  
35 des méthodes indicelles. *Bull. Mens. la Société linnéenne Lyon* 76, 255–268. <https://doi.org/10.3406/linly.2007.13667>
- 36 Korfali, S. I. and Davies, B.E., 2003. A comparison of metals in sediments and water in the river Nahr-Ibrahim, Lebanon: 1996 and  
37 1999. *Environ. Geochem. Health* 25, 41–50.
- 38 Kulkarni, S.J., Deshbhandari, P.G., Jayappa, K.S., 2015. Seasonal Variation in Textural Characteristics and Sedimentary  
39 Environments of Beach Sediments , Karnataka Coast , India. *Aquat. Procedia* 4, 117–124.  
40 <https://doi.org/10.1016/j.aqpro.2015.02.017>
- 41 Lakkis, S., 2018. Le phytoplancton des eaux marines libanaises et du bassin levantin. *Biologie, Biodiversité, biogéographie*, 2nd ed.  
42 Publications de l'Université Libanaise.
- 43 Li, Y., Zhang, H., Tu, C., Fu, C., Xue, Y., Luo, Y., 2016. Sources and fate of organic carbon and nitrogen from land to ocean:  
44 Identified by coupling stable isotopes with C/N ratio. *Estuar. Coast. Shelf Sci.* 181, 114–122.  
45 <https://doi.org/10.1016/j.ecss.2016.08.024>
- 46 Liu, D., Li, X., Emeis, K.C., Wang, Y., Richard, P., 2015. Distribution and sources of organic matter in surface sediments of Bohai  
47 Sea near the Yellow River Estuary, China. *Estuar. Coast. Shelf Sci.* 165, 128–136. <https://doi.org/10.1016/j.ecss.2015.09.007>
- 48 Lorenzen, C.J., 1967. Determination of chlorophyll and pheopigments: Spectrophotometric equations. *Limnol. Oceanogr.* 12, 343–  
49 3446.
- 50 M.A., 2010. Détermination du carbone organique total dans les solides: dosage par titrage. Québec.

- 1 Magni, P., Abe, N., Montani, S., 2000. Quantification of microphytobenthos biomass in intertidal sediments: layer-dependant  
2 variation of chlorophyll-a content determined by spectrophotometric and HPLC methods. *La Mer* 38, 57–63.
- 3 Magni, P., Montani, S., 2006. Seasonal patterns of pore-water nutrients, benthic chlorophyll a and sedimentary AVS in a  
4 macrobenthos-rich tidal flat. *Hydrobiologia* 571, 297–311. <https://doi.org/10.1007/s10750-006-0242-9>
- 5 Manivel, T., Mukesh, M., Chandrasekaran, A., Rajmohan, R., Immauel David, T., Premkumar, R., 2016. Studies on textural  
6 characteristics of sediments in Lower Gadilam River, Cuddalore District, Tamilnadu, India. *Int. J. Adv. Res.* 4, 694–705.
- 7 McComb, A.J., Qiu, S., Lukatelich, R.J., McAuliffe, T.F., 1998. Spatial and temporal heterogeneity of sediment phosphorus in the  
8 Peel-Harvey Estuarine System. *Estuar. Coast. Shelf Sci.* 47, 561–577. <https://doi.org/10.1006/ecss.1998.0389>
- 9 Mcheik, A., Fakh, M., Trabulsi, H., Toufaily, J., Hamieh, T., Garnier-Zarli, E., Bousserhine, N., 2015. Metal Pollution Assessment of  
10 Sediment and Water in Al-Ghadir River: Role of Continuously Released Organic Matter and Carbonate and Their Purification  
11 Capacity. *Int. J. Environ. Monit. Anal.* 3, 162–172. <https://doi.org/10.11648/j.ijema.20150303.18>
- 12 MOE/UNDP/ECODIT, 2011. State and trends of the Lebanese environment. Third édition.
- 13 Mohan, P.M., 2000. Sediment transport mechanism in the Vellar estuary, east coast of India. *Indian J. Mar. Sci.* 29, 27–31.
- 14 Nakhlé, K., 2003. Le mercure, le cadmium et le plomb dans les eaux littorales libanaises: apports et suivi au moyen de bio-  
15 indicateurs quantitatifs (éponges, bivalves et gastéropodes). Université Paris 7.
- 16 Nehme, N., Haydar, C., Koubaissy, B., Fakh, M., Awad, S., Toufaily, J., Villieras, F., Hamieh, T., 2014. Metal concentrations in river  
17 water and bed sediments of the Lower Litani River Bassin, Lebanon. *J. Adv. Chem.* 8, 12p.
- 18 Padhi, D., Singarasubramanian, S.R., Panda, S., Venkatesan, S., 2017. Depositional Mechanism as Revealed from Grain size  
19 Measures of Rameswaram Coast, Ramanathapuram District, Tamil Nadu, India. *Int. J. Theor. Appl. Sci.* 9, 168–177.
- 20 Passega, R., 1964. Grain Size Representation by Cm Patterns as a Geological Tool. *J. Sediment. Petrol.* 34, 830–847.
- 21 Pruski, A.M., Buscail, R., Bourrin, F., Vétion, G., 2019. Influence of coastal Mediterranean rivers on the organic matter composition  
22 and reactivity of continental shelf sediments: The case of the Têt River (Gulf of Lions, France). *Cont. Shelf Res.* 181, 156–  
23 173. <https://doi.org/10.1016/j.csr.2019.05.009>
- 24 Pusceddu, A., Bianchelli, S., Gambi, C., Danovaro, R., 2011. Assessment of benthic trophic status of marine coastal ecosystems :  
25 Signi fi cance of meiofaunal rare taxa. *Estuar. , Coast. Shelf Sci.* 93, 420–430. <https://doi.org/10.1016/j.ecss.2011.05.012>
- 26 Pusceddu, A., Sara, G., Armeni, M., Fabiano, M., Mazzola, A., 1999. Seasonal and spatial changes in the sediment organic matter  
27 of a semi-enclosed marine system (W-Mediterranean Sea). *Hydrobiologia* 397, 59–70.
- 28 Quiros-Collazos, L., Pedrosa-Pàmies, R., Sanchez-Vidal, A., Guillén, J., Duran, R., Cabello, P., 2017. Distribution and sources of  
29 organic matter in size-fractionated nearshore sediments off the Barcelona city ( NW Mediterranean ). *Estuar. , Coast. Shelf*  
30 *Sci.* 189, 267–280. <https://doi.org/10.1016/j.ecss.2017.03.004>
- 31 Rajganapathi, V.C., Jitheshkumar, N., Sundararajan, M., Bhat, K.H., Velusamy, S., 2013. Grain size analysis and characterization of  
32 sedimentary environment along Thiruchendur coast, Tamilnadu, India. *Arab. J. Geosci.* 6, 4717–4728.  
33 <https://doi.org/10.1007/s12517-012-0709-0>
- 34 Ramesh, G., Ramkumar, T., Mukesh, M. V, 2015. A Study on the Textural Characteristics of Arasalar River Estuary Sediments of  
35 Karaikal, East Coast of India. *Int. J. Recent Sci. Res.* 6, 2779–2782.
- 36 Ranjan, R.K., Routh, J., Ramanathan, A.L., Klump, J.V., 2011. Elemental and stable isotope records of organic matter input and its  
37 fate in the Pichavaram mangrove-estuarine sediments (Tamil Nadu, India). *Mar. Chem.* 126, 163–172.  
38 <https://doi.org/10.1016/j.marchem.2011.05.005>
- 39 Saad, Z., Kazpard, V., Geyh, M.-A., Slim, K., 2004a. Chemical and isotopic composition of water from springs and wells in the  
40 Damour river basin and the coastal plain in Lebanon. *J. Environ. Hydrol.* 12.
- 41 Saad, Z., Slim, K., Khalaf, G., EL Samad, O., 2004b. Impacts des rejets des eaux résiduaires sur la qualité physico-chimique et  
42 algologique du Nahr Antélias. *Bull. la Société neuchâteloise des Sci. Nat.* 127, 69–82.
- 43 Sahu, B.K., 1964. Depositional Mechanisms from the Size Analysis of Clastic Sediments. *J. Sediment. Petrol.* 34, 73–83.
- 44 Sanlaville, P., 1977. Étude géomorphologique de la région du littoral du Liban.
- 45 Schubert, C.J., Nielsen, B., 2000. Effects of decarbonation treatments on delta13C values in marine sediments. *Mar. Chem.* 72-,  
46 55–59.
- 47 Sondi, I., Lojen, S., Juracic, M., Prohic, E., 2008. Mechanisms of land – sea interactions – the distribution of metals and sedimentary  
48 organic matter in sediments of a river-dominated Mediterranean karstic estuary. *Estuar. , Coast. Shelf Sci.* 80, 12–20.  
49 <https://doi.org/10.1016/j.ecss.2008.07.001>

- 1 Stevenson, F.J., Cheng, C.-N., 1970. Amino acids in sediments: Recovery by acid hydrolysis and quantitative estimation by a  
2 colorimetric procedure. *Geochim. Cosmochim. Acta* 34, 77–88.
- 3 Tarabay, R., 2011. Vers un projet sociétal libanais ... L'environnement durable : une nouvelle citoyenneté ? Université Paris IV-  
4 Sorbonne.
- 5 Thomas, R.L., Shaban, A., Khawlie, M., Kawass, I., Nssouli, B., 2005. Geochemistry of the sediments of the El Kabir River and  
6 Akkar watershed in Syria and Lebanon. *Lakes Reserv. Res. Manag.* 10, 127–134.
- 7 Tselepidis, A., Polychronaki, T., Marrale, D., Akoumaniaki, I., Dell'Anno, A., Pusceddu, A., Danovaro, R., 2000. Organic matter  
8 composition of the continental shelf and bathyal sediments of the Cretan Sea (NE Mediterranean). *Prog. Oceanogr.* 46, 311–  
9 344.
- 10 Wang, C., Lv, Y., Li, Y., 2018. Riverine input of organic carbon and nitrogen in water-sediment system from the Yellow River estuary  
11 reach to the coastal zone of Bohai Sea, China. *Cont. Shelf Res.* 157, 1–9. <https://doi.org/10.1016/j.csr.2018.02.004>
- 12 Wang, K., Chen, J., Jin, H., Li, H., Zhang, W., 2018. Organic matter degradation in surface sediments of the Changjiang estuary:  
13 Evidence from amino acids. *Sci. Total Environ.* 637–638, 1004–1013. <https://doi.org/10.1016/j.scitotenv.2018.04.242>
- 14 Winogradow, A., Pempkowiak, J., 2018. Characteristics of sedimentary organic matter in coastal and depositional areas in the Baltic  
15 Sea. *Estuar. Coast. Shelf Sci.* 204, 66–75. <https://doi.org/10.1016/j.ecss.2018.02.011>
- 16 Zhang, Q., Blomquist, J.D., 2018. Watershed export of fine sediment , organic carbon , and chlorophyll-a to Chesapeake Bay :  
17 Spatial and temporal patterns in 1984 – 2016. *Sci. Total Environ.* 619–620, 1066–1078.  
18 <https://doi.org/10.1016/j.scitotenv.2017.10.279>
- 19 Zhong, Y., Chen, Z., Li, L., Liu, J., Li, G., Zheng, X., Wang, S., Mo, A., 2017. Bottom water hydrodynamic provinces and transport  
20 patterns of the northern South China Sea: Evidence from grain size of the terrigenous sediments. *Cont. Shelf Res.* 140, 11–  
21 26. <https://doi.org/10.1016/j.csr.2017.01.023>
- 22 Zhu, C., Wang, Z., Xue, B., Yu, P., Pan, J., Wagner, T., Pancost, R.D., 2011. Characterizing the depositional settings for  
23 sedimentary organic matter distributions in the Lower Yangtze River-East China Sea Shelf System. *Estuar. Coast. Shelf Sci.*  
24 93, 182–191. <https://doi.org/10.1016/j.ecss.2010.08.001>
- 25

|   |    |
|---|----|
| <b>Table 1:</b> Description of sampling stations .....  | 8  |
| Table 2: Linear discriminant functions to differentiate among environment of depositions .....  | 11 |
| <b>Table 3: Geochemical and biochemical results</b> .....   | 21 |
|   |    |
| <b>Figure 1:</b> A: Ibrahim River watershed and Dams location (Khalaf, 1984).....   | 7  |
| <b>Figure 2:</b> Sampling stations distribution at Ibrahim River coastal marine area.....   | 9  |
| <b>Figure 3:</b> Grain size Class weight distribution (A), Mean vs Sorting (B), Mean vs Skewness (C), at the different sampling stations. ....  | 16 |
| <b>Figure 4:</b> Ternary Diagram representing the grain size distribution (A) and the C-M Plot (B) for the sampling stations.....   | 17 |
| <b>Figure 5:</b> Linear Discriminate Function (LDF) Plots (A: Y3 vs Y2, B: Y4 vs Y3) and spatial distribution of Y3 (C) at the studied area .....   | 18 |
| <b>Figure 6:</b> Spatial distribution of OC (%) (A), TN (%) (B) and Mud (%) (C) at the Studied area..   | 20 |
| <b>Figure 7:</b> Chlorophyll spatial distribution (A) and Labile organic matter percentages (LOM) spatial distribution(B) at the studied area .....   | 22 |
| <b>Figure 8:</b> $\delta^{13}\text{C}$ ranges and associated organic matter sources (A) and Spatial distribution of the terrestrial fraction (B) at Ibrahim River coastal marine area ..... | 23 |
| <b>Figure 9: Organic composition and grain size distribution in surface sediments A:</b><br>Correlation Matrix (N=38 K=36 r=0.324, p<0.05; r=0.418, p<0.01; r= 0.518, p<0.001) .....        | 32 |

# PCA - Biplot

